



**ADDIS ABABA UNIVERSITY
SCHOOL OF GRADUATE STUDIES
FACULTY OF TECHNOLOGY
DEPARTMENT OF CIVIL ENGINEERING**

**CONSTITUTIVE MODEL
FOR
THE RED CLAY SOILS OF ADDIS ABABA**

**A Thesis Submitted to the School of Graduate Studies of
Addis Ababa University in Partial Fulfillment of the Requirements for the Degree of
Master of Science in Civil Engineering**

Tezera Firew

**Advisor:
Dr.-Ing. Girma Boled**

July, 2003



**ADDIS ABABA UNIVERSITY
SCHOOL OF GRADUATE STUDIES
FACULTY OF TECHNOLOGY
DEPARTMENT OF CIVIL ENGINEERING**

**CONSTITUTIVE MODEL
FOR
THE RED CLAY SOILS OF ADDIS ABABA**

Tezera Firew

July, 2003

Approved by Board of Examiners

_____ Advisor	_____ Signature	_____ Date
_____ External Examiner	_____ Signature	_____ Date
_____ Internal Examiner	_____ Signature	_____ Date
_____ Chairman	_____ Signature	_____ Date

ACKNOWLEDGEMENT

I would like to express my most sincere gratitude to Dr. –Ing. Girma Boled for careful guidance and suggestions provided throughout the course of this research.

My special thanks go to Amarebih Refera for the help that you provided without limit. I am grateful to my friends Adane A., Berhanu A., Daniel N., Dawit H., Dereje A., Esayas G., Firew F., Riyad A., Samson T., and Zelalem for your support.

I would also like to thank my mother Hiwot Kifetew, my brother Eskinder, my sisters Tigist and Netsanet for their support and encouragement. Jerry, I thank you.

Dedicated to My Father

Firew Azmatch

TABLE OF CONTENTS

	Page
List of Symbols	vii
List of Figures	viii
Abstract	ix
1.INTRODUCTION	1
1.1 General	1
1.2 Scope and Objectives of the Present Study	2
2. LITERATURE REVIEW	4
2.1 General	4
2.2 Fundamentals of Plasticity Theory	4
2.2.1 Yield Criterion	5
2.2.2 Normality Rule	8
2.2.3 Plastic Stability	9
2.2.4 Stress-Elastic Strain Relationship	15
2.2.5 Evolution Rule	16
2.3 Classification of Hardening Rules	16
2.3.1 Isotropic Hardening	17
2.3.2 Kinematic Hardening	17
2.3.3 Anisotropic Hardening	20
2.4 Review Of Existing Models	22
2.4.1 Classical Plasticity	22
2.4.2 Critical State Models	25
2.4.3 Cap Models	27
2.4.4 Single Surface Plasticity Models	29

3. THE PROPOSED MODEL	33
3.1 General	33
3.2 Assumptions	34
3.3 Polynomial Representation of Yield Functions	34
3.4 The Model	36
4. DETERMINATION OF MATERIAL CONSTANTS	42
4.1 General	42
4.2 Soil Testing Program	42
4.3 Procedure for Evaluating Material Constants	43
4.3.1 Elastic Constants: E, ν	43
4.3.2 Ultimate State Parameters: β, γ, m	44
4.3.3 Phase Change Parameter: n	46
4.3.4 Constants for Hardening: $\beta_a, \eta_1, \beta_b, \eta_2$	47
4.4 Material Constants for the Red Clay Soils of Addis Ababa	51
5. VALIDATION OF THE MODEL	52
5.1 General	52
5.2 Model Validation	52
6. CONCLUSIONS AND RECOMMENDATIONS	63
APPENDIX	65
LIST OF REFERENCES	74

LIST OF SYMBOLS

E	Young's modulus
G	Shear modulus
J_1, J_2, J_3	Invariants of the stress tensor
J_{2D}, J_{3D}	Invariants of the deviatoric stress tensor
K	Bulk modulus
p	Mean stress
q	Deviator stress
$\varepsilon_1, \varepsilon_2, \varepsilon_3$	Principal strains
ε^e	Elastic strain
ε^p	Plastic strain
ε_{ij}^p	Plastic strain tensor
$d\varepsilon_{ij}^e$	Elastic part of the total incremental strain
$d\varepsilon_{ij}^p$	Plastic part of the total incremental strain
$d\varepsilon_{kk}^p$	Incremental volumetric plastic strain
$d\varepsilon_{ij}^p$	Incremental deviatoric plastic strain tensor
ξ	Total plastic strain trajectory
ξ_D	Deviatoric part of ξ
ξ_V	Volumetric part of ξ
ν	Poisson's ratio

LIST OF FIGURES

FIGURE	PAGE
2.1 Typical Uniaxial Stress-Strain Response in Elastoplastic Deformation	6
2.2 Stable and Unstable Plastic Materials (Uniaxial Stress)	10
2.3 Schematic of the Incremental Stress and the Incremental Plastic Strain Vectors in the Hyper Stress Space	13
2.4 Schematic of the Development of Nonassociative Behavior for frictional Materials	14
2.5 Schematic of the Isotropic Hrdening Rule for Uniaxial Stress-Strain Response	
2.6 Schematic of the Kinematic Hrdening Rule for Uniaxial Stress-Strain Response	19
2.7 Schematic of the Anisotropic Hrdening Rule for Uniaxial Stress-Strain Response	21
2.8 Classical yield Criteria for Soils	23
2.9 Coulomb Criterion	24
2.10 Drucker-Prager Criterion	25
2.11 Cam-Clay Yield Surfaces in Triaxial Plane	26
2.12 The Three- Dimensional View of the Modified Cam-Clay Model by Roscoe and Burland (1968)	27
2.13 Drucker-Prager Tyep of Strain Hrdening Cap Model	28
2.14 Plot of F in $\sqrt{J_{2D}}$ - J_1 Space	29
3.1 Plot of the Yield Surfaces on $\sqrt{J_{2D}}$ - J_1 Space	40
3.2 Plot of the Yield Surfaces on the Triaxial Plane	41
5.1 Comparison of Stress – Strain Curves for a Test ($\sigma_3' = 220\text{Kpa}$) used to find the Material Constants	54
5.2 Comparison of Stress – Strain Curves for a Test ($\sigma_3' = 250\text{Kpa}$)	

used to find the Material Constants	55
5.3 Comparison of Stress – Strain Curves for a Test ($\sigma_3' = 210\text{Kpa}$)	
used to find the Material Constants	56
5.4 Comparison of Stress – Strain Curves for a Test ($\sigma_3' = 190\text{Kpa}$)	
not used to find the Material Constants	57
5.5 Comparison of Stress – Strain Curves for a Test ($\sigma_3' = 180\text{Kpa}$)	
not used to find the Material Constants	58
5.6 Comparison of Stress – Strain Curves for a Test ($\sigma_3' = 190\text{Kpa}$)	
not used to find the Material Constants	59
5.7 Comparison of Stress – Strain Curves for a Test ($\sigma_3' = 110\text{Kpa}$)	
not used to find the Material Constants	60
5.8 Comparison of Stress – Strain Curves for a Test ($\sigma_3' = 190\text{Kpa}$)	
not used to find the Material Constants	61
5.9 Comparison of Stress – Strain Curves for a Test ($\sigma_3' = 250\text{Kpa}$)	
not used to find the Material Constants	62
A.1 Plot of pore pressure (u) Vs. axial strain (ϵ_1) corresponding to Fig.5.1	65
A.2 Plot of pore pressure (u) Vs. axial strain (ϵ_1) corresponding to Fig.5.2	66
A.3 Plot of pore pressure (u) Vs. axial strain (ϵ_1) corresponding to Fig.5.3	67
A.4 Plot of pore pressure (u) Vs. axial strain (ϵ_1) corresponding to Fig.5.4	68
A.5 Plot of pore pressure (u) Vs. axial strain (ϵ_1) corresponding to Fig.5.5	69
A.6 Plot of pore pressure (u) Vs. axial strain (ϵ_1) corresponding to Fig.5.6	70
A.7 Plot of pore pressure (u) Vs. axial strain (ϵ_1) corresponding to Fig.5.7	71
A.8 Plot of pore pressure (u) Vs. axial strain (ϵ_1) corresponding to Fig.5.8	72
A.9 Plot of pore pressure (u) Vs. axial strain (ϵ_1) corresponding to Fig.5.9	73

ABSTRACT

Key words: constitutive equations, strains, stress, elastic-plastic theories.

An associative constitutive model originally developed by C. S. Desai based on rate-independent elastoplasticity concepts is validated for the Red Clay Soils of Addis Ababa. The basic concept of the model used herein was proposed and developed by Desai (1980). The yield function is expressed in terms of the state of stress, while the evolution or strain hardening process is characterized by using internal state variables such as the irreversible strain.

Laboratory tests are conducted to determine the material constants. The material constants that are associated with the model are found based on four different states of a material deformation process: the elastic, plastic accompanied by hardening, phase change from contraction to dilation and the ultimate state.

The model is then validated by comparing predictions with laboratory tests from which the constants were found, and also with tests not used for finding the constants. Comparison of observed and predicted response show that the model yielded predictions that compared remarkably well with the observed behavior.

Chapter 1

INTRODUCTION

1.1 General

The motion of a continuum is governed by such principles as the law of conservation of mass, conservation of momenta, first and second laws of thermodynamics. These laws are applicable to a material regardless of its internal constitution. If mechanical energy is the only form of energy of interest in a problem, then the energy equation is merely the first integral of the equation of motion. If the interactions of thermal and mechanical processes are significant, then the equation of energy contains a thermal energy term and is an independent equation to be satisfied. For an isothermal case, the equation of continuity and motion constitute four equations for ten unknown functions of time and positions; namely density ρ , the three velocity components V_i (or displacement U_i) and the six independent stress components given by stress tensor, σ_{ij} . Further restrictions would have to be introduced before the motion of a continuum can be determined. One group of such additional restrictions comes from the statement of the mechanical behavior of the medium in the form of a specification of stress-strain relationship. These relationships are called "constitutive equations".

There are several groups of constitutive theories. The aim of each theory is to represent the behavior of a certain class of materials under some ideal conditions. The linear elastic theory based on Hooke's law, for example, describes responses of those materials for which a stress-free initial state exists and stress is a unique linear function of strain. Theory of plasticity, on the other hand, describes rate independent inelastic behavior of materials.

The progress in stress and displacement analysis of soil-structure systems using elastic stress-strain models has been seriously limited by difficulties in modeling several important features of the soil behavior. While general stress-strain nonlinearity could be

incorporated into elastic models in a satisfactory manner, the feature associated with stress path dependency and dilatancy are much more difficult to deal with.

Plasticity theory, on the other hand, has been one of the most popular vehicles for developing nonlinear constitutive relations for geologic materials. Although numerous constitutive models are available at this time, none of these models are general enough to characterize behavior of a class of materials under complex loading conditions. For example the associated flow requirement based on classical plasticity produces an overestimation of plastic volume increase, which tends to increase the pressure in the material, and because of its pressure sensitivity, to increase its strength in an unrealistic manner. So for frictional materials, use of nonassociated flow rule has to be introduced to account for the problem of shear-induced dilatancy; this, however, renders the constitutive matrix nonsymmetric.

The primary goal of the present study is to validate a constitutive model, based on the associative law of plasticity, for Red Clay soils of Addis Ababa.

1.2 Scope and Objectives of the Present Study

Analysis of soil-structure interaction problems is generally complex and in most cases, closed-form solutions are not readily available. This is mainly due to the complexities and nonlinear and inelastic characteristics of soils. The interaction effects of soil and structure further complicate the problem. As a result, numerical methods are often used for the analysis of this class of problems. Among the various numerical schemes available, the finite element method has been recognized as one of the most versatile because of its capability of capturing and incorporating into the formulation many salient complexities of a problem; this includes material nonlinearity, geometric nonlinearity, complex boundary condition, and loadings.

Advantage gained through formulating a complex problem using the finite element technique cannot be properly exploited if an appropriate solution algorithm is not available. Efficient numerical techniques and solution algorithms alone, however, are not

sufficient to provide realistic answers to complex soil-structure interaction problems. Since the response of most geologic materials is highly nonlinear, a proper constitutive law must be developed which can capture the salient features of a 'system' throughout the realm of its deformation process.

Use of nonlinear elastic models can account for a very limited class of materials; it falls short in adequately taking into account stress path dependency and dilatant behavior during shear deformation. However, models based on the theory of plasticity can describe rate independent nonlinear and inelastic response of materials. Thus, constitutive laws based on the theory of plasticity can be effectively used to characterize the behavior of geological material.

The accuracy of the solution of a boundary value problem with a given constitutive model is highly dependent upon the values of the material constants associated with the model. As a result, appropriate laboratory test are necessary to determine these constants.

The objectives of the present work are:

- i.) To propose and validate an associative plasticity based model for the red clay soils of Addis Ababa.
- ii.) To determine the material constants for the model using laboratory test data for red clay soils of Addis Ababa.
- iii.) To verify the proposed constitutive model with respect to the laboratory test data.

Chapter 2 of this paper is dedicated to describing some basic ideas underlying the theory of plasticity and to the general review of some of the existing plasticity models. Chapter 3 is devoted to the development of the proposed model. Chapter 4 is devoted to describing various steps that are involved in evaluating the material parameters. Chapter 5 is devoted to verifying the model with respect to the laboratory test data. Finally, conclusions and recommendations will be presented in chapter 6.

CHAPTER 2

LITERATURE REVIEW

2.1 General

Elasticity, plasticity and viscosity are three broad based material response phenomena upon which stress-strain laws are developed. But fundamental distinctions exist between elasticity, viscosity and plasticity.

Elastic materials are those whose relations between stress and strain are reversible. Linear elasticity applies when the relation is linear. Viscous materials are those whose stress-strain relations involve time. For example, the strain response to an applied constant stress might increase over a period of time. Linear viscoelasticity implies that the relation between stress and strain is linear for equal values of time, but the dependence of either stress or strain on time is usually nonlinear.

Plasticity, on the other hand, is a branch of the constitutive theory that describes the time independent nonlinear and inelastic behavior of materials. The usual example involves application and removal of a prescribed stress and observation of some unrecovered strain after the cycle is complete. However, viscoplasticity involves description of nonlinear material response that varies with time.

2.2 Fundamentals of Plasticity Theory

Four different facets are involved in the formulation of a constitutive law based on the theory of plasticity:

- i) Yield criterion

- ii) Normality rule
- iii) Stress-elastic strain relationship
- iv) Evolution or hardening rule.

2.2.1 Yield Criterion:

The concept of a yield surface, yield criterion or yield function, F , is central to the plasticity theory. A material is said to yield at a point when a scalar condition, expressed as a function of stress, signifies initiation of irreversible inelastic response.

In the case of a material subjected to uniaxial state of stress, Fig. 2.1, the yield function can be expressed as

$$F = \sigma - \sigma_y = 0 \tag{2.1}$$

Where σ is the present state of stress and σ_y is the stress level where initiation of yielding takes place. From Eq. (2.1), if $\sigma = \sigma_y$, $F = 0$ and the material is undergoing plastic strains. If $\sigma < \sigma_y$, $F < 0$, the behavior is elastic.

For a multiaxial state of stress, nine components of stress are involved at a material point. While some of these components are increasing, the remainder of them could be decreasing. So construction of a yield function for a multiaxial state of stress should include all nine components of stress given by the stress tensor, σ_{ij} . Besides stresses, a yield expression may be a function of plastic work W^p , deformation (strain) history, ϵ^p_{ij} , and other tensor or scalar valued internal variable. Therefore, F can be expressed as

$$F = F(\sigma_{ij}, \epsilon^p_{ij}, W^p, \alpha_{ijk}, a_1, a_2, \dots, a_N) \tag{2.2}$$

α_{ijk} , is a tensor valued internal variable and a_i ($i = 1, 2, \dots, N$) are scalar valued internal variables. These internal variables can physically be related to some micro damage of the material matrix.

The equality (2.2) is valid for a mechanical system under isothermal condition. For a thermomechanical state, provision must be made to include the influence of temperature.

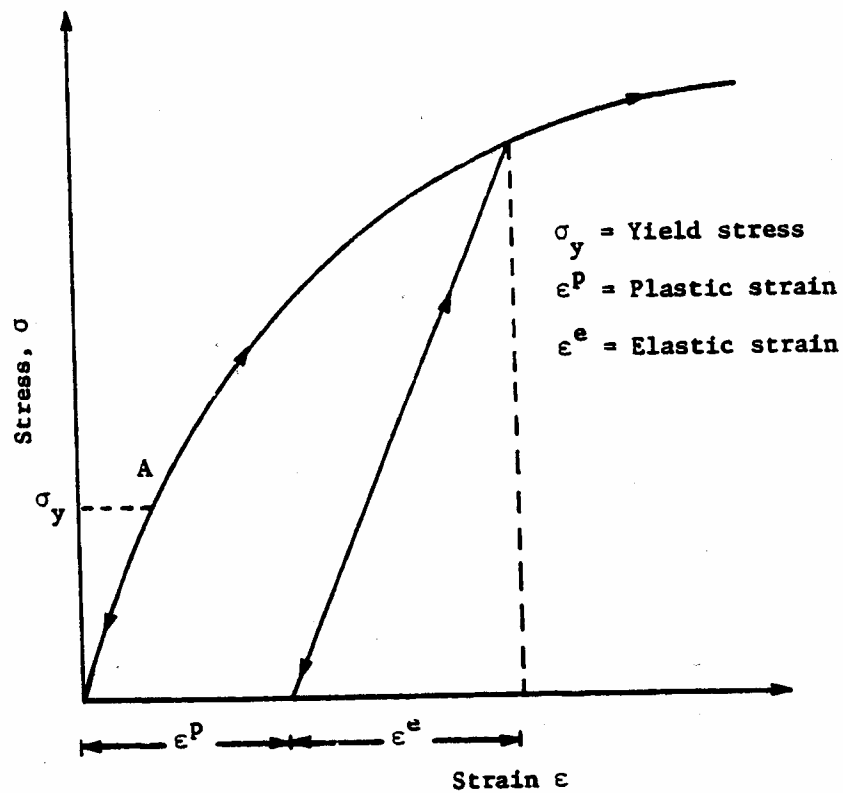


Figure 2.1 Typical Uniaxial Stress-Strain Response in Elastoelastic Deformation (Hashmi, 1987)

For a constitutive law to represent material behavior adequately, certain physical and mathematical requirements should be satisfied. These are called the axioms of continuum mechanics (Hashmi, 1987). Proof of satisfaction of all axioms by a constitutive theory is a formidable task. Details of these axioms are beyond the scope of this paper.

If a material is assumed to be homogeneous, a yield function is valid everywhere in a material. Eq. (2.2) can be expressed in terms of the principal stresses and their directions; that is,

$$F = F(\sigma_1, \sigma_2, \sigma_3, n_1, n_2, n_3) \quad (2.3)$$

Where σ_1 , σ_2 and σ_3 are the principal stresses, and n_1 , n_2 and n_3 are their direction cosines. Eq. (2.3) can be simplified if an assumption is made regarding material properties. If we assume that the material is isotropic, then it does not have any preferred directions.

Therefore, the yield criterion in Eq. (2.3) can be expressed only in terms of principal stresses; that is, for an isotropic material:

$$F = F(\sigma_1, \sigma_2, \sigma_3) \quad (2.4)$$

The principal stresses are physical quantities whose values do not depend on the coordinate system in which the components of stress were initially given. They are, therefore, invariants of the stress state, invariants with respect to rotation of the coordinate axes to which the stresses are referred. So Eq. (2.4) can be conveniently expressed in terms of the invariants

$$F = F(J_1, J_2, J_3) \quad (2.5)$$

$$J_1 = \sigma_{ii}$$

$$J_2 = \frac{1}{2} (\sigma_{ij} \sigma_{ji}) \quad (2.6)$$

$$J_3 = \frac{1}{3} \sigma_{ij} \sigma_{jk} \sigma_{ki}$$

In classical theory of plasticity, the yield function, F , and the plastic potential, Q , are assumed to be equal. The incremental plastic strains are then proportional to the gradient of F . This is called the “associative” law in plasticity. Description of material behavior based on the associative law has been found to be appropriate for a certain class of materials, especially those which are not pressure-sensitive.

For some frictional materials, however, formulation of a constitutive relation based on the assumption that $F = Q$ does not conform well to observed behavior. The incremental plastic strains are, therefore, not associated with the yield surface F . This is predominantly reflected through excessive prediction of dilatant behavior. To overcome this, it is necessary to extend plasticity theory to a ‘nonassociated’ form in which the plastic

potential, Q , and yield surfaces, F , are defined separately. The incremental plastic strain is then evaluated based on the plastic potential, Q .

2.2.2 Normality Rule

Normality rule, often called flow rule, defines the incremental plastic strains $d\epsilon_{ij}^p$. In the theory of plasticity, incremental plastic strains are defined by assuming the existence of a function, Q , called the plastic potential. The directions of the plastic strain rates or increments are classically governed by the plastic potential, Q , so that increments of plastic strain, $d\epsilon_{ij}^p$, are proportional to the gradient of the plastic potential. Introducing a constant of proportionality, λ , $d\epsilon_{ij}^p$ can be expressed as (Hashmi, 1987)

$$d\epsilon_{ij}^p = \lambda * \frac{\partial Q}{\partial \sigma_{ij}} \quad (2.7)$$

where $\lambda \geq 0$.

In the simplest case, the plastic potential and the yield function are the same. For strain hardening and softening materials, the factor λ in Eq. (2.7) can be computed from the hardening or softening rule. For perfectly plastic materials, it may be indeterminate, or it may be found from requirements of compatibility with elastic strains.

2.2.3 Plastic Stability

In terms of the plastic work done by the incremental stress during an increment of plastic deformation, Drucker's definition of a stable plastic material is a generalization of the following stability considerations in a uniaxial stress test (Hashmi, 1987).

Figure 2.2 (a) shows a curve of true tensile stress T versus natural strain q for a work-hardening material such that for any plastic deformation increment, the change dT in the stress is positive.

Figure 2.2 (b) shows the same stresses plotted against plastic strain q^p . The rising curve denotes a stable work-hardening while in Fig. 2.2 (c), from point T_1 on, the curve drops so that further plastic strain occurs at smaller stresses, a clearly unstable situation.

Drucker formulated the material stability definition in terms of the work done by the stress increments on the plastic deformation increments. For the increment dq^p shown in fig. 2.2 (b), the total plastic work is $\int T_1 dq^p$, equal to the area of strip ABCD. But the major part of this area; namely, ABED, is the work done by the stress T_1 at which the increment began; the smaller area DEC is the work by the stress increment dT . In the stable case $dT dq^p > 0$, while in the unstable case $dT dq^p < 0$ so that the total plastic work is less than would have been done by constant stress T_1 . For a perfectly plastic material, we would have the neutral condition, $dT dq^p = 0$ (Hashmi, 1987).

Now Drucker's stability postulates can be phrased as follows:

- i) The plastic work done by the external agency during the application of the additional stresses is positive, and
- ii) The net work performed by the external agency during the cycle of adding and removing stresses is nonnegative.

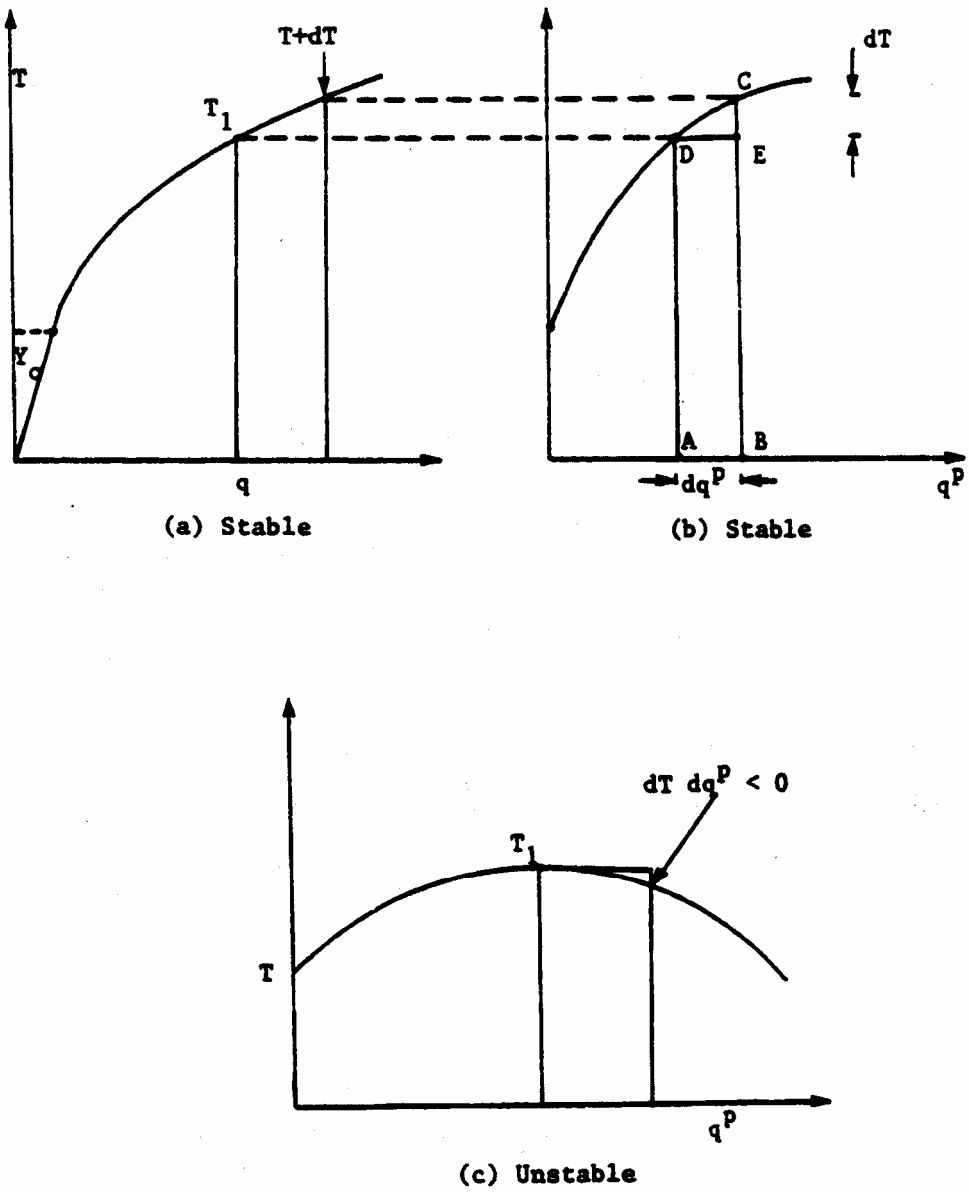


Figure 2.2 Stable and Unstable Plastic Materials (Uniaxial Stress) (Hashmi, 1987)

Consequences of Drucker's Postulates (Hashmi, 1987):

There are two major consequences of the stability postulates defined above. They are:

- i) The yield surface, when plotted in the stress hyperspace, must be a convex hyper surface.
- ii) The incremental plastic strain, $d\epsilon_{ij}^p$, should be normal to the yield surface at the loading point. Discussion on the proof of these consequences can be found in Desai and Siriwardane.

Figure 2.3 represents the effect of Drucker's postulates. For any stress $d\sigma_{ij}$, the yield surface is convex and tangential at the point R to AB. The incremental plastic strain $d\epsilon_{ij}^p$ is normal to the yield surface at the loading point. Thus, if F is a yield surface, the incremental plastic strain, $d\epsilon_{ij}^p$, is proportional to the gradient of F; that is

$$d\epsilon_{ij}^p = \lambda \frac{\partial F}{\partial \sigma_{ij}} \quad (2.8)$$

Comparing Eq. (2.8) with Eq. (2.7), it is found $F = Q$. But the plastic potential, Q, may not be identical to F. This gives rise to two kinds of plasticity formulations: (a) Associative plasticity, where it is assumed that $F = Q$, and (b) Non-associative plasticity, where $F \neq Q$ (Desai and Faruque, 1983; Frantziskonis et al, 1986).

The phenomenon of nonassociative behavior exhibited by frictional materials can be explained as follows. Consider a yield surface F on the stress-space (Fig. 2.4). An arbitrary increment of stress, $d\sigma_{ij}$, is applied at the point A which causes plastic strain. The direction of incremental plastic strain depends on the gradient of F at point A. But based on the assumptions of classical theory of plasticity, this increment of plastic strain $d\epsilon_{ij}^p$ is normal to the yield surface. However for pressure-sensitive materials, there will be a frictional deformation, $d\epsilon_{ij}^{fp}$, in the direction normal to the incremental stress $d\sigma_{ij}$. So

the two incremental strains, $d\varepsilon_{ij}^p$, which is normal to the yield surface, and $d\varepsilon_{ij}^{fp}$, which is normal to the incremental stress, will produce the resultant, $d\varepsilon_{ij}^{fp}$. This is then no longer perpendicular to the yield surface F . Hence, constitutive law based on the associative law of plasticity is not appropriate to define the actual observed behavior of frictional materials. If, however, the plastic potential Q and the yield surface F are assumed to be different then the resultant incremental plastic strain $d\varepsilon_{ij}^{fp}$ can be considered to be normal to the plastic potential Q . So it is appropriate to develop constitutive relation for frictional materials based on the nonassociative law of plasticity where $F \neq Q$ and derive the incremental plastic strains as being normal to the plastic potential, Q .

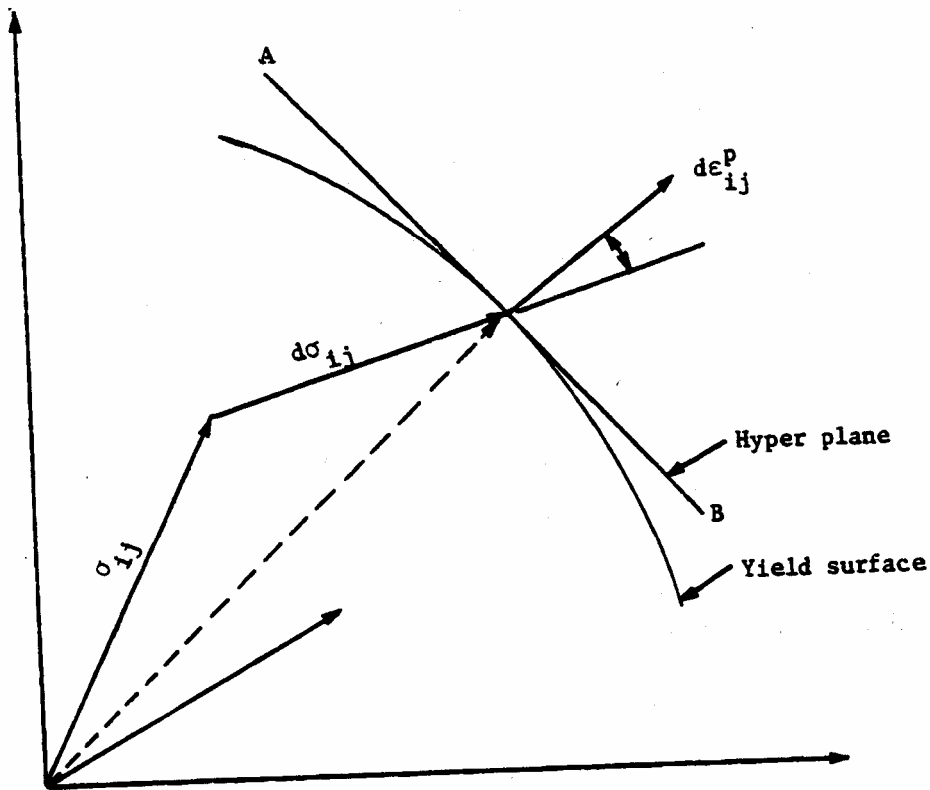


Figure 2.3 Schematic of the Incremental Stress and the Incremental Plastic Strain Vectors in the Hyper Stress Space (Hashmi, 1987)

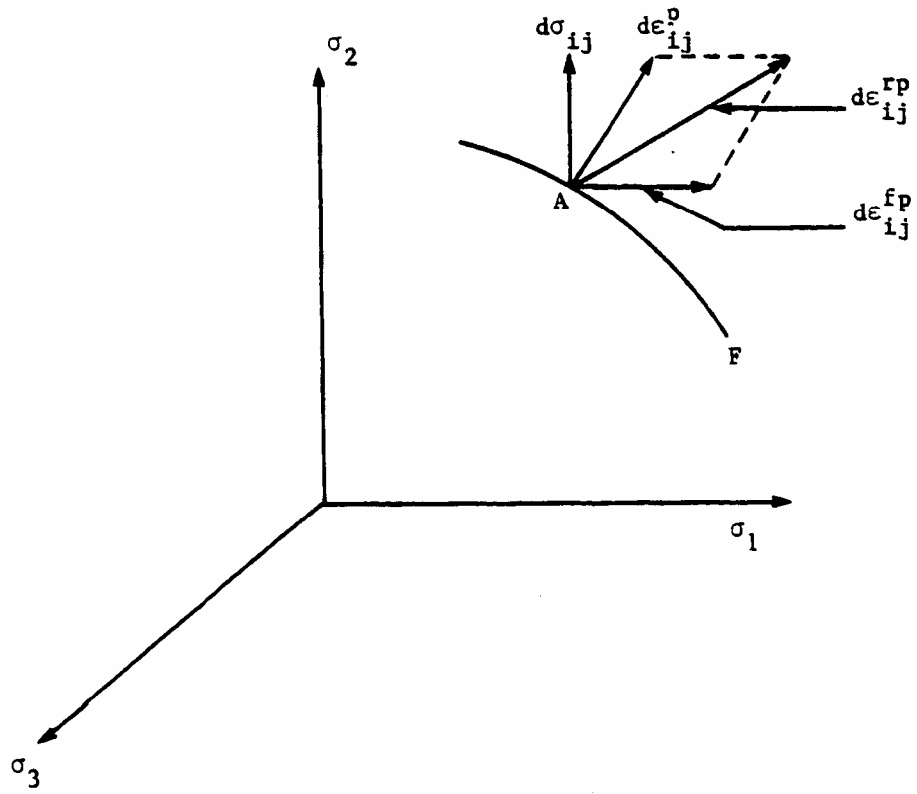


Figure 2.4 Schematic of the Development of Nonassociative Behavior for Frictional Materials (Hashmi, 1987)

2.2.4 Stress-Elastic Strain Relationship

When subjected to any arbitrary loading, a material point, on reaching the plastic limit, begins to flow (deform) under a constant state of stress; that is, the plastic strain occurs without any increase of stress. Thus, at any point, the stress cannot be related to the total strain, but only to the elastic part of the total strain. Since the stress-strain relations are nonlinear and inelastic, piecewise linearity is assumed and the incremental stress is related to the incremental elastic strain through the generalized Hooke's law

$$d\sigma_{ij} = C_{ijkl} d\epsilon_{kl}^e \quad (2.9)$$

where $d\sigma_{ij}$ = incremental stress, $d\epsilon_{ij}^e$ = elastic part of the total incremental strains, and C_{ijkl} = elastic constitutive relation tensor.

A basic assumption made in the development of stress-strain relations for elastic-plastic materials is the small deformation concept. Then for each load increment the corresponding strain increment can be decomposed into elastic and plastic components; that is,

$$d\epsilon_{kl} = d\epsilon_{kl}^e + d\epsilon_{kl}^p \quad (2.10)$$

Using Eqs. (2.7) and (2.8), the incremental stress $d\sigma_{ij}$ can be expressed as

$$d\sigma_{ij} = C_{ijkl} (d\epsilon_{kl} - d\epsilon_{kl}^p) \quad (2.11)$$

Equation (2.11) is the basis for explicit development of the stress-strain relations.

2.2.5 Evolution Rule

A material point is plastically stable if the stress at that point is a monotonic function of the strain (Hashmi, 1987). Except for the perfect plastic material, most materials exhibit increase of strength beyond the elastic limit. This phenomenon is called work or strain hardening. According to Hashmi (1987), Hill (1950) attributed such behavior to the micro-structural rearrangements and locking of the progressive failure during plastic deformations. Hardening rules, which are also known as evolution rules, are intended to define the process of strength gain in a material due to permanent straining. Some materials also show loss in strength during the deformation process. This is called the strain softening behavior. The degradation associated with strain-softening can be considered to be caused by disruption in the internal constitution of the material due to formation of discontinuities such as microcracks, fractures and voids. Hence a softening material may no longer be continuous, and a plasticity model that is based on the theory of continua may not be strictly applicable. An alternative is to combine the continuum model with appropriate modifications to allow for the discontinuities. Evolution of the softening process can then be defined through some internal variable (Desai et al., 1986; Frantziskonis and Desai, 1986). This aspect is not considered herein.

2.3 Classification of Hardening Rules:

In the theory of plasticity, there are three types of hardening rules:

- i) Isotropic hardening
- ii) Kinematic hardening
- iii) Anisotropic hardening

Explanation of these hardening processes is given below.

2.3.1 Isotropic Hardening:

In this hardening process, it is assumed that the yield surface expands uniformly about the center in the stress space. There is no rigid body rotation or translation of the yield surface. Fig. 2.5 shows the hardening process for a material subjected to a uniaxial state of stress.

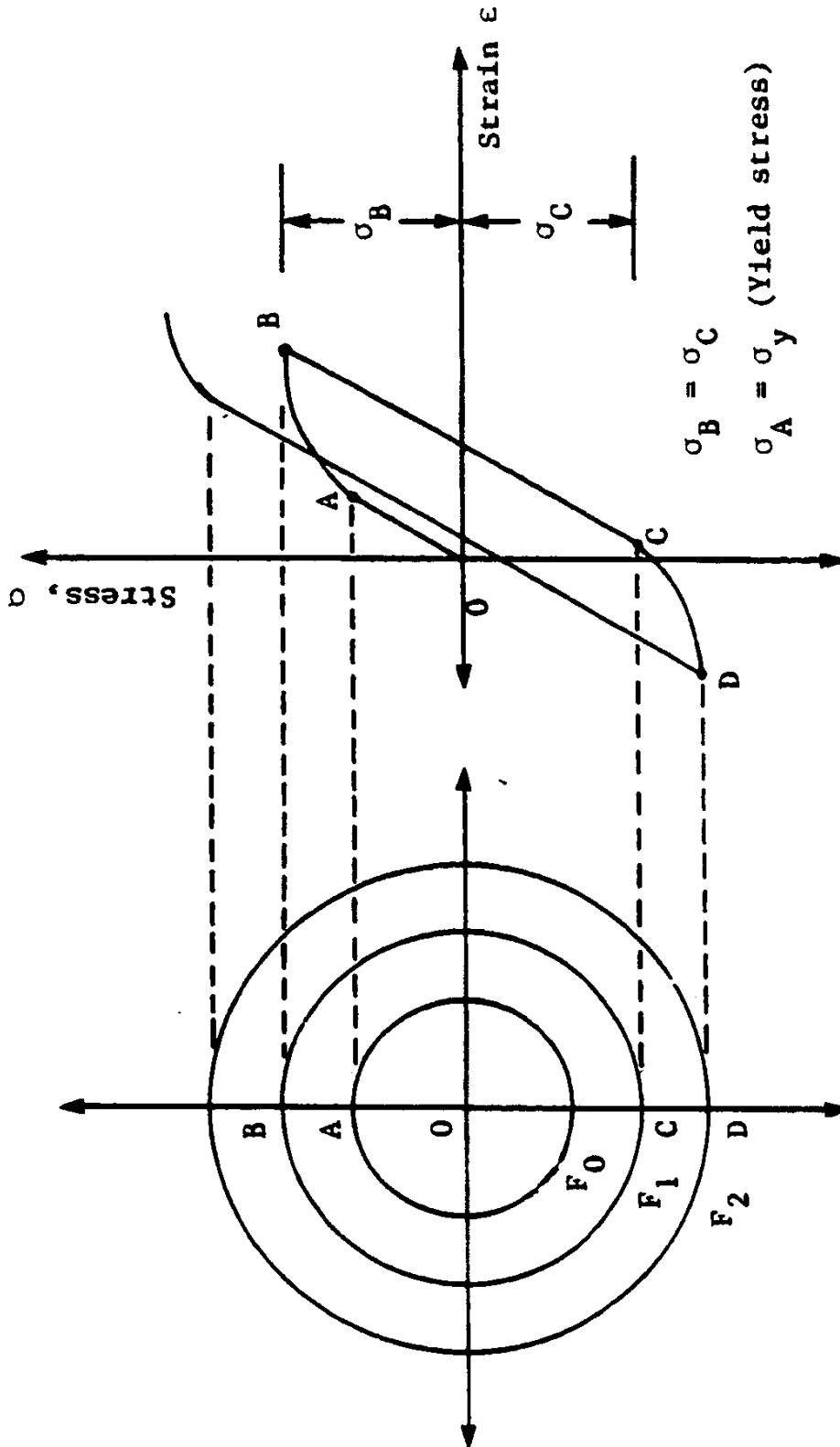


Figure 2.5 Schematic of the Isotropic Hardening Rule for Uniaxial stress-Strain Response (Hashmi, 1987)

The point A on the stress-strain curve represents the elastic limit. Any stress increment will not cause plastic strain unless the stress reaches the yield surface F_0 corresponding to the point A. Further application of stress will cause A to move to B, causing the yield surface F_0 to expand uniformly to F_1 about the origin O. On unloading from point B, and continued in the reverse direction, the material point behaves elastically until it reaches point C, such that $|\sigma_B| = |\sigma_C|$. From point C up to D, plastic deformation again sets in, and the yield surface expands to F_2 . This continuous loading and unloading increases the elastic limit. A real material, however, starts yielding in the reverse loading before point C is reached. This phenomenon is known as the Baughinger effect (Hashmi, 1987). The disadvantage of the isotropic hardening rule is that it cannot take into account the Baughinger effect. However, for monotonic loading, isotropic hardening is adequate to describe material behavior.

2.3.2 Kinematic Hardening:

According to Hashmi(1987), Ishlinsky (1959) and Prager (1955, 1956) introduced the kinematic hardening rule. It is assumed that the yield surface translates in the stress space as a rigid body during the plastic deformation. For a uniaxial stress-strain case, Fig. 2.6, with kinematic hardening, initial yielding starts when the stress reaches point A and the corresponding yield surface position is F_0 . With increase of stress from A to B, the yield surface moves along to its new position F_1 . Upon unloading from point B, the deformation is elastic until the stress point reaches point C, which is diametrically opposite to the point B. In this case, $\sigma_c < \sigma_b$. Further reverse loading from point C causes the yield surface to translate along with the stress point to its new location, F_2 , causing further plastic strain. Though kinematic hardening rules predict Baughinger effect, the yielding in reverse loading starts much too soon, which may not be the case with real materials.

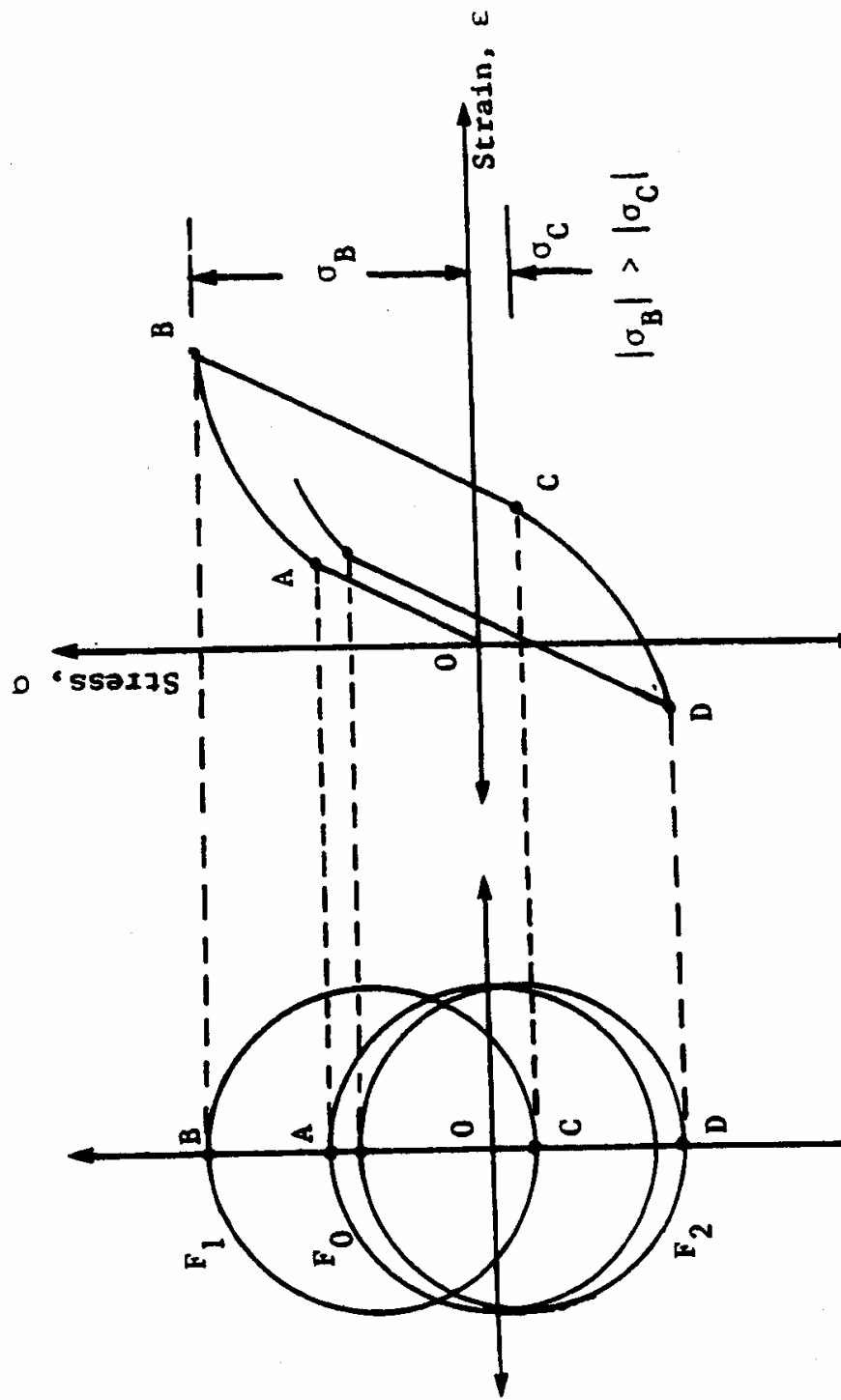


Figure 2.6 Schematic of the Kinematic Hardening Rule for Uniaxial stress-Strain Response (Hashmi, 1987)

2.3.3 Anisotropic Hardening:

A yield surface can experience a combination of isotropic and kinematic hardening, which can be termed anisotropic hardening. Here, it is assumed that the yield surface expands and translates simultaneously with the shape remaining the same (Hashmi, 1987). Fig. 2.7 shows the uniaxial representation of an anisotropic hardening rule. Point A on the stress-strain curves represents the elastic limit and the corresponding yield surface, F_0 . Upon loading from A to B, the yield surface translates to its new position B and becomes F_1 . The radius of the surface also changes from R_0 to R_1 . Unloading from point B produces no further plastic strain until the stress point reaches C., corresponding to the yield surface F_1 , but diametrically opposite to point B. Further reverse loading to point D will cause the yield surface to expand and, at the same time, translate downward. At point D, the yield surface becomes F_2 . Since plastic deformation is irreversible, the expansion of the yield surface is monotonic; i.e., the sizes of the yield surfaces monotonically increase. Referring to Fig. 2.7, it may be represented by the following condition: $R_0 < R_1 < R_2 < R_3 \dots \dots \dots < R_n$, where $R_0, R_1, R_2, R_3 \dots \dots \dots < R_n$ denote the sizes of the yield surfaces $F_0, F_1, F_2, \dots \dots \dots F_n$. However, during this process, the shape of the yield surface remains the same. Anisotropic hardening rule is found to take the Bauehinger effect into account better than kinematic hardening rule.

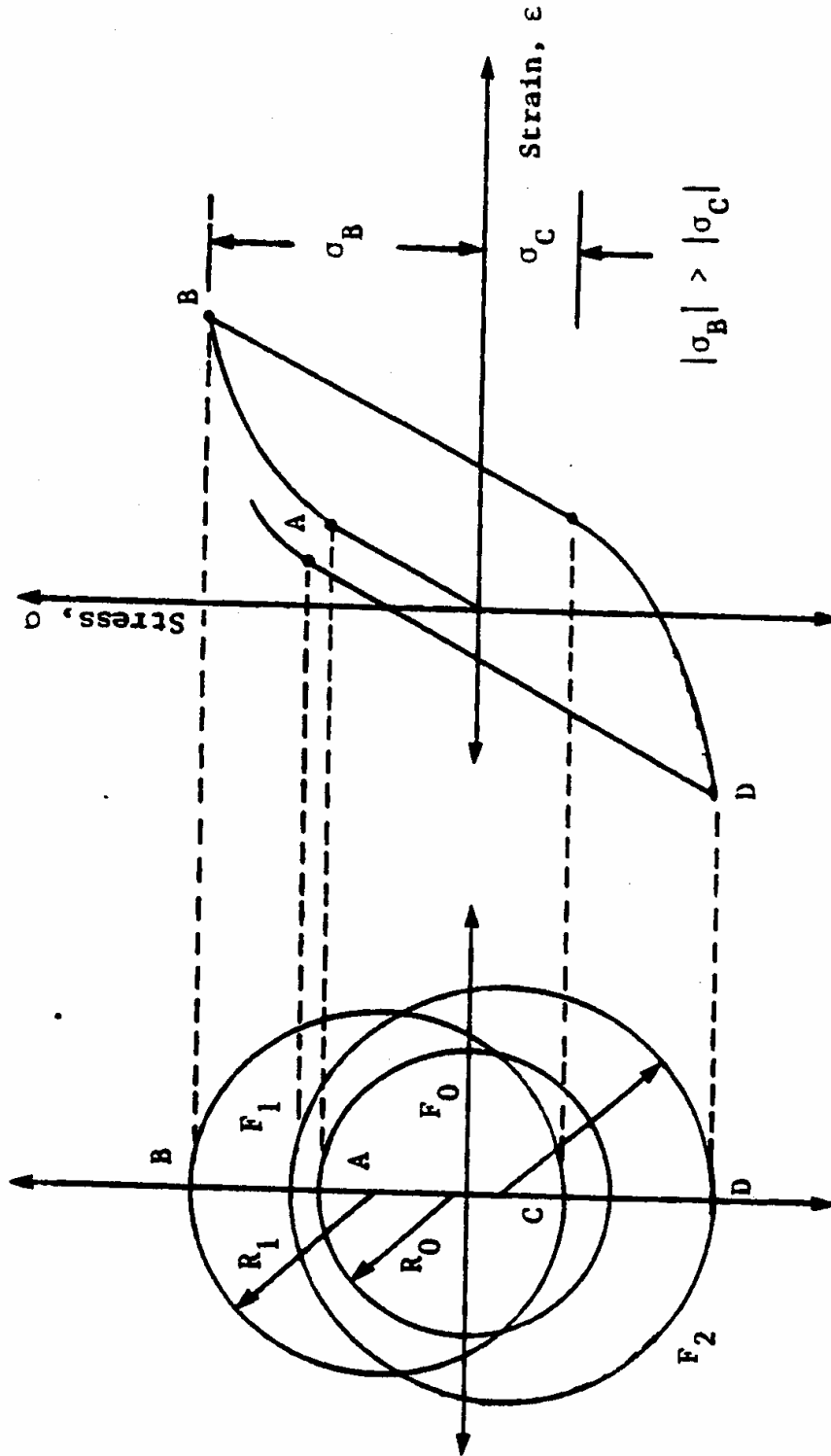


Figure 2.7 Schematic of the Anisotropic Hardening Rule for Uniaxial stress-Strain Response (Hashmi, 1987)

2.4 Review of Existing Models

In the following review of existing models, it is not intended to provide a detailed review of the large body of literature, and only brief description of the models will be presented.

2.4.1 Classical Plasticity

In classical plasticity, the failure surface is adopted as the yield surface, F , when the state of stress reaches that surface. A state of stress below the failure surface denotes elastic behavior. Thus one failure surface defines the yielding of the material. The classical Tresca, von Mises, Mohr-Coulomb and Drucker-Prager Criteria fall into this category, in which F is expressed in terms of J_{2D} and or J_1 , and material constants, cohesion (C) and/or angle of friction, Φ , related to failure, here J_1 is the first invariant of the stress tensor, σ_{ij} and J_{2D} is the second invariant of the deviatoric stress tensor, S_{ij} .

Tresca and von Mises Models:

The von Mises criterion considers the effect of intermediate principal stress on the yield strength, while the Tresca criterion neglects this principal stress and considers only the maximum shear stress. Because of the possible numerical complications required for the corner treatment along the edges of the Tresca hexagon, the von Mises criterion is mathematically more convenient for practical use. Since both criteria are developed primarily for metals whose yield strength is insensitive to the hydrostatic pressure, they are not generally suitable for application to stability problems in soil mechanics. To include the effect of the hydrostatic pressure on soil strength, the Tresca and von Mises criteria were extended to the so-called extended Tresca and extended von Mises criteria. These extended criteria in the principal stress space are sketched in Fig. 2.8.

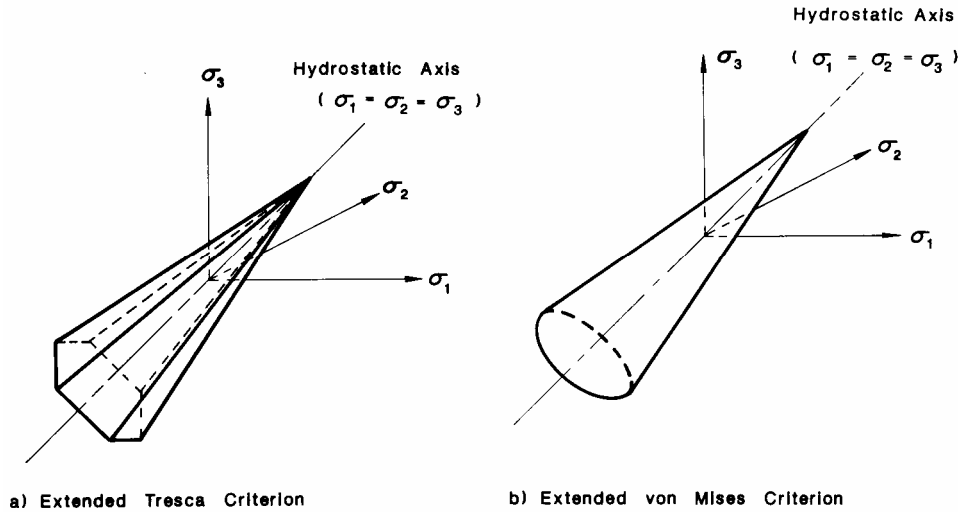


Figure 2.8 Classical yield criteria for soils (Chen and Mizuno, 1990)

Coulomb Model

The Coulomb criterion is certainly the best known failure criterion in soil mechanics. This criterion, which was proposed for geotechnical materials much earlier than the Tresca and von Mises yield criteria for metals, is the first type of failure criterion that takes into consideration the effect of hydrostatic pressure on the strength of granular materials. This criterion states that failure occurs when the shear stress τ and the normal stress σ acting on any element in the material satisfy the linear equation:

$$|\tau| + \sigma \tan(\phi) - c = 0 \quad (2.12)$$

where c and Φ denote the cohesion and angle of internal friction, respectively.

The Coulomb's failure criterion is an irregular hexagonal pyramid in the principal stress space (Fig. 2.9). Eventhough the Coulomb criterion is simple; the Coulomb surface exhibits corners or singularities in three-dimensional generalization. The resulting general

yield or failure function with singularities gives rise to some difficulties in numerical analysis. In addition to these limitations, the Coulomb criterion neglects the effect of intermediate principal stress on shear strength. Nevertheless, for the most part, this criterion has in the past been used for necessity and simplicity to obtain reasonable solutions to important and practical problems in geotechnical engineering.

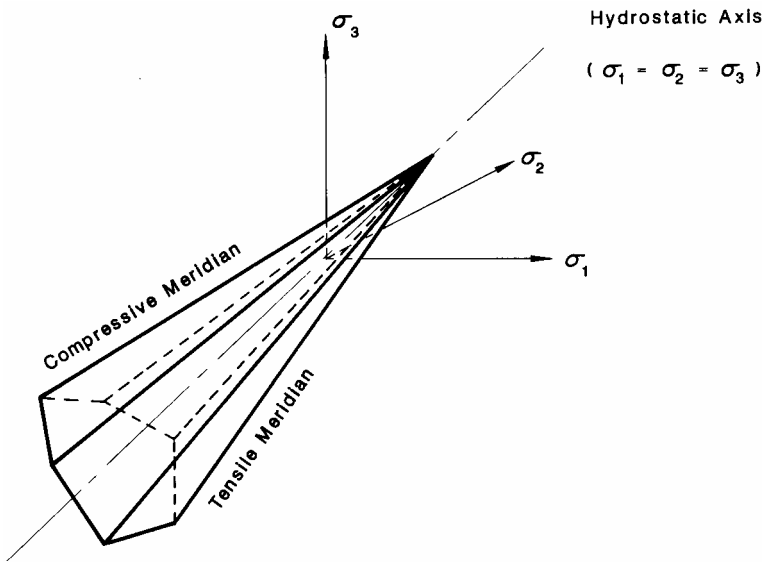


Figure 2.9 Coulomb Criterion (Chen and Mizuno, 1990)

Drucker-Prager Model:

The Drucker-Prager perfectly plastic model (Chen and Mizuno, 1990), which neglects the influence of J_{3D} on the cross-sectional shape of failure surface, can be considered as the first attempt to approximate the well-known Coulomb criterion by a simple smooth function. This criterion is expressed as a simple invariant function of the first invariant of stress tensor, J_1 , and the second invariant of deviatoric stress tensor, J_{2D} , together with two material constants α and k . It has the simple form:

$$F = \sqrt{J_{2D}} - \alpha J_1 - K = 0 \quad (2.13)$$

The yield or failure surface of the above equation in the principal stress space depicts a right circular cone with the symmetry about the hydrostatic axis (Fig. 2.10).

The Drucker-Prager model cannot predict plastic volumetric strain or compaction of soil materials during hydrostatic loading. To improve this limitation, an extended von Mises model with a convex end cap was proposed by Drucker et al. (Chen and Mizuno, 1990). However, the failure surface of this model results in a much higher prediction of dilatancy than that observed in experiments

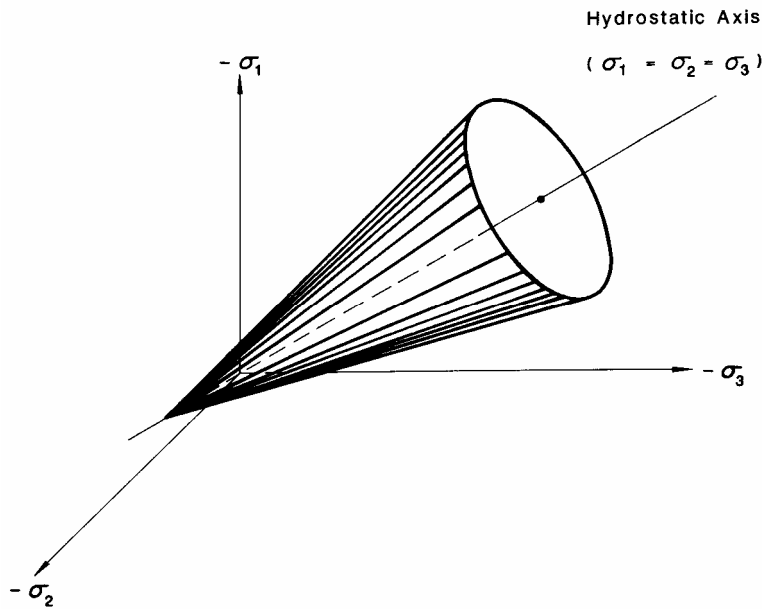


Figure 2.10 Drucker-Prager Criterion (Chen and Mizuno, 1990)

2.4.2 Critical State Models

In the critical state concept proposed by Roscoe and coworkers, a yield function F_y defines the continuous yielding, while the final yield locus is defined by the critical state at which no volume change occurs during further shearing. The locus of the critical state points, F_c , defines the critical state line (CSL). The surface F_y represents a single surface; however, the model involves two surfaces, a part of F_y below F_c , and F_c for description of the entire behavior.

Cam-Clay Model

The Cam-clay model, for normally consolidated and lightly overconsolidated clays, was developed at the Cambridge University to predict the response of remolded specimens subjected to drained or undrained triaxial compression tests. Since their development, the Cam-clay models have been extended to general three-dimensional analysis with some success. The formulation does not allow for an adequate treatment of the strain-softening behavior of heavily overconsolidated clays.

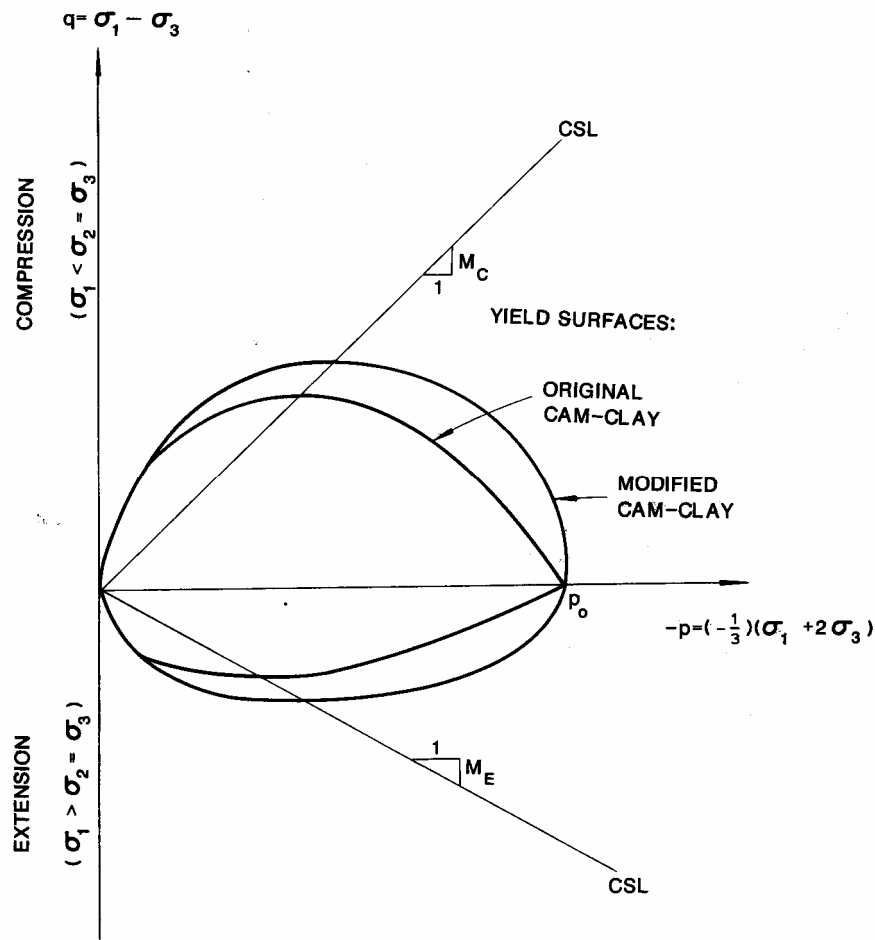


Figure 2.11 Cam-Clay Yield Surface in Triaxial Plane (Chen and Mizuno, 1990)

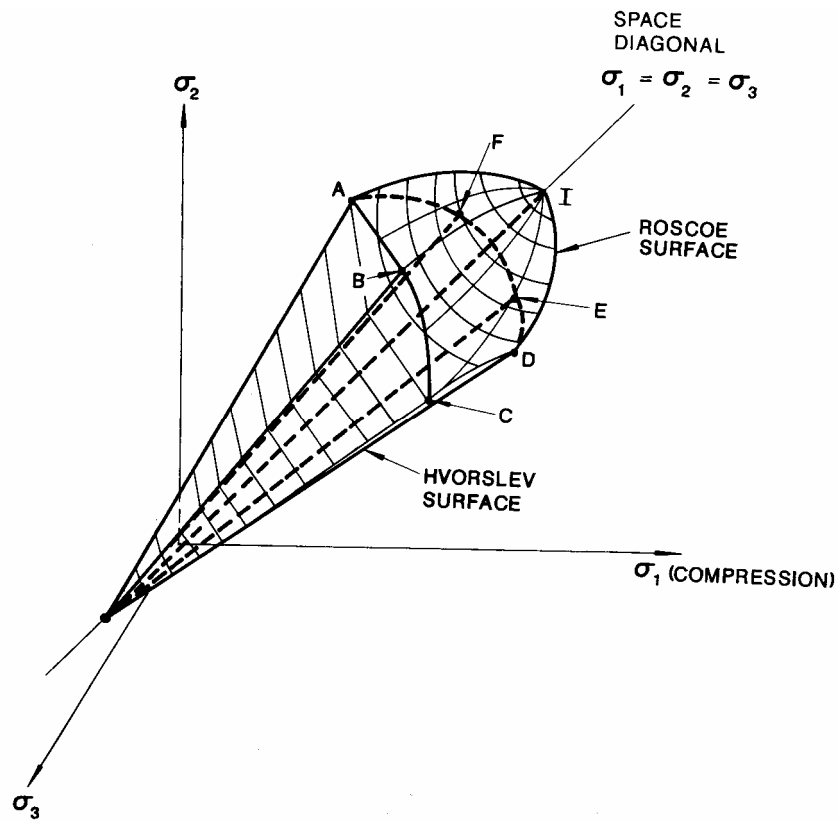


Figure 2.12 The three-dimensional view of the modified cam-clay model by Roscoe and Burland, 1968 (Chen and Mizuno, 1990)

2.4.3 Cap Models

The cap model, proposed by DiMaggio and Sandler is similar to the critical state model, except that a composite failure yield surface F_1 replaces the CSL. Again, the yield surfaces F_y allows for continuous yielding, and at failure, F_1 is used as separate yield surface.

The critical state and cap models can suffer from various limitations:

- i) For states of stresses below the CSL, only compressive volumetric strains are predicted, and dilative strains are predicted only if F_c is used as yield surface.

Since many materials exhibit volume increase (dilation) before the critical state or peak stress is reached, the model cannot predict such behavior;

- ii) The yield surface is circular in the principal stress space; hence, the model cannot allow for path dependent failure or ultimate response, as it occurs for many geologic materials;
- iii) The hardening or yielding is defined through total volumetric plastic strains (or void ratio), thus the definition of hardening does not include the effect of deviatoric plastic strains;
- iv) The yield surface, F_y , intersects the p-axis orthogonally. Hence, the coupled effect of the mean pressure on shear strains is not included; and
- v) If F_c (or F_1) is used in computations, the model involves singularity at the intersection of F_y and F_c (or F_1), which may cause computational difficulties.

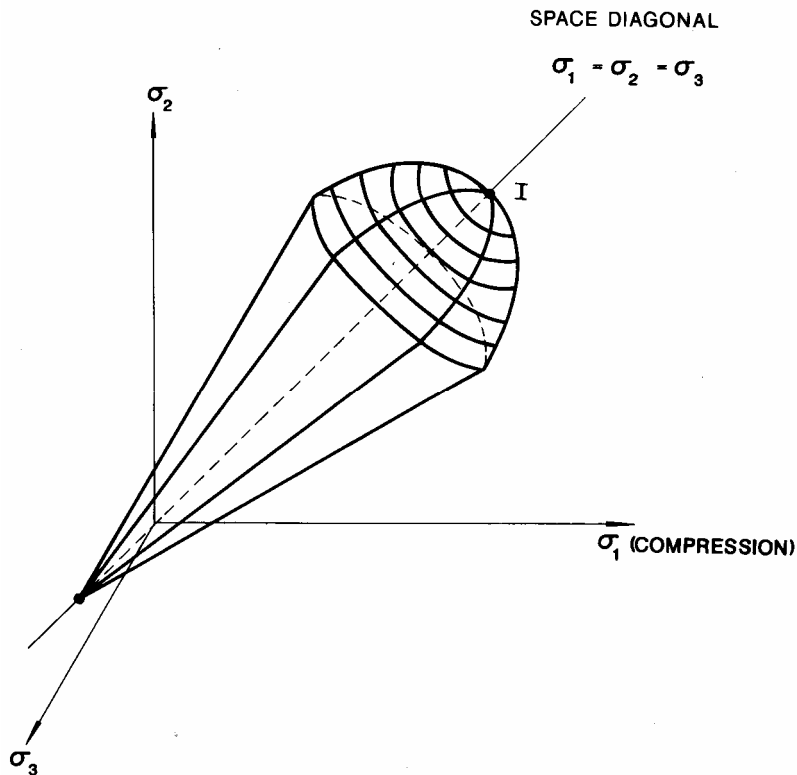


Figure 2.13 Drucker-Prager type of strain hardening cap model (Chen and Mizuno, 1990)

2.4.4 Single Surface Plasticity Models

A single surface plasticity model involves a single mathematical function for describing yielding of a geological material. Thus, the same function defines the entire process of yielding from the start of loading upto failure peak or ultimate condition, and includes the portions above and below the phase change curve, Fig 2.8, that defines the state where volume change transits from contraction to dilation. The final or ultimate state is defined through the final yield surface (F_u) corresponding to the asymptotic states of stress from the observed stress-strain behavior. It provides unique ultimate state towards which deformation process approaches, and the conventionally defined failure, peak or critical states lie below the ultimate state coincide with it.

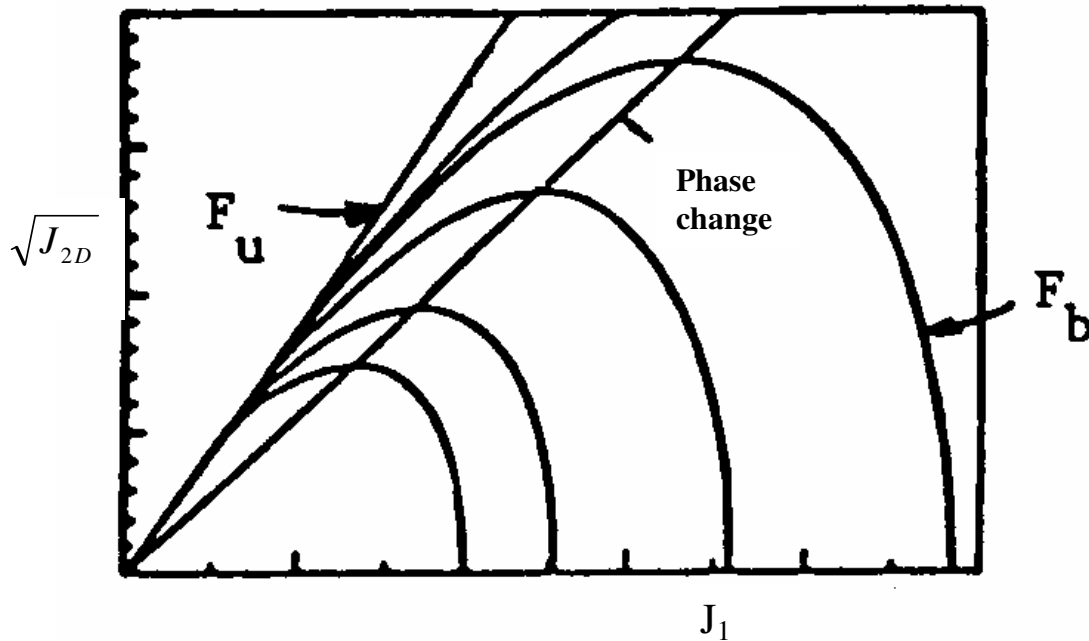


Figure 2.14 Plot of F in $\sqrt{J_{2D}}$ - J_1 space (Desai and Gioda, 1990)

Lade and Kim Model

Lade and Kim have proposed what is referred to as the single hardening constitutive models. This approach is considered similar to the hierarchical single surface (HISS) approach developed previously by Desai and co-workers, Fig. 2.14 (Desai and Gioda, 1990).

Lade and Kim model is based on a number of factors that were considered by Desai and co-workers in their HISS approach that integrates both theoretical and experimental aspects. There are some minor differences, however. For example, (1) Lade and Kim approach defines separate failure surface, which in the HISS approach is a subset of the compact single surface function, and (2) the number of constants required is greater than that in the HISS approach, and (3) the damage/softening response in the HISS approach is based on a consistent definition of damage function that leads to incorporation of damage due to microcracking and discontinuous nature of the material damage and subsequent softening, whereas in the Lade and Kim approach, softening is incorporated in the continuum sense involving contraction of the yield surface.

Hierarchical Single Surface (HISS) Models

Around 1975, Desai and co-workers considered the foregoing models, and implemented some of them in nonlinear finite element procedures for static, dynamic and consolidation analysis of problems in geomechanics (Desai and Gioda, 1990). However, in view of the limitations mentioned, systematic research that integrates theoretical, experimental and verification phases was initiated so as to develop a unified approach for modeling of geologic materials. In the HISS approach progressively refined higher grades of models can be developed based on simple and basic category. One of the ingredients of this hierarchical approach has been development of a single mathematical function for yield

and potential functions. In the HISS approach, the yield function F and plastic potential, Q , are expressed as a complete polynomial in J_1 , $J_2^{1/2}$ and $J_3^{1/3}$.

In addition to removing the forgoing limitations of the critical state and cap models, the HISS approach includes the following considerations (Desai and Gioda, 1990):

- i) Theoretical basis in conjunction with the form invariance principle leading to development of models for special attributes of materials from a generalized and unified concept, referred to as the hierarchical approach. The concept is capable of handling both solid materials and the discontinuities (interfaces and joints).
- ii) Development of nonassociative models based on the correction of F to lead to the potential function, Q .
- iii) Development of the hardening function in terms of the total trajectory of plastic strains, ξ , including deviatoric and volumetric components; in the original critical state and cap models, hardening is defined only in terms of the volumetric plastic strains. Here it was found that use of the trajectory of total plastic strains provides more consistent relationships than the use of plastic work, W^P . It may be noted that the yield surfaces F are related to and are functions of plastic work contours. In other words, it can be shown that, in general, the plastic work contours have the same form and follow the yield surfaces.
- iv) The final yield surface corresponds to the unique ultimate state; thus ambiguities due to the use of various definitions such as peak and failure are avoided.
- v) The concept allows for easy incorporation of the change in the shape and size of F , and tension and cohesion of materials.
- vi) Development of as simple a model as possible with optimal number of material constants with appropriate physical meanings. As a result, the number of constants involved in the associative (δ_0) and nonassociative (δ_1) models is smaller or equal to other models of comparable capabilities.

- vii) Extensive cylindrical triaxial and multiaxial laboratory tests on soils, rocks and concrete have been performed to define the constants in models together with development of guidelines for minimum number of test required for evaluation of the constants.
- viii) Verification of the models with respect to laboratory tests used to find the constants and those not used to find the constants, and implementation of the models on nonlinear finite element procedures for two- and three-dimensional static and dynamic analysis including verification of the numerical procedures with respect to laboratory and field observations for various boundary value problems. Here, one of the advantages is that the single surface avoids the singularity that exists in the two and multisurface models.
- ix) The HISS approach allows for the development models of progressively increased complexities such as nonassociative behavior (δ_1), anisotropic hardening with fluid pressure (δ_{2+p}), damage and softening (δ_{0+r}) and viscoplastic (δ_{0+vp}) models, based on corrections of the basic δ_0 -model that defines behavior of isotropic material, hardening isotropically associative plasticity.

Based on the above discussion, the HISS concept is chosen for this work.

CHAPTER 3

THE PROPOSED MODEL

3.1 General

There has been a great deal of progress made in the development and understanding of the constitutive relations for soils. There is substantial overlap between the models, particularly where the anisotropic, strain hardening and nonassociated flow rule plasticity theories are concerned. There is no one best model. Each model may work best for a material (application) for which it was developed, and it may not work for other materials.

A large number of plasticity models are available. But one of the major shortcomings of all these models is that the yielding and ultimate surfaces are expressed by separate yield functions involving a point of intersection or discontinuity. This may give rise to nonuniqueness of the normals at the point of intersection. Thus the increment of the plastic strain is not defined at the point of intersection of the two surfaces. This problem, however, can be overcome by defining the entire deformation process through evolution of a single yield function.

The basic concept of the model used herein was proposed and developed by Desai (1980). The general hierarchical approach that includes the model used herein as a special case is described by Desai et al. (1986). In the hierarchical approach, a basic constitutive

equation is evolved first, based on the associative law of classical plasticity. The nonassociative model is then obtained by applying a correction to the basic constitutive equation. This approach eliminates the necessity of defining a separate plastic potential, Q , to capture the nonassociative behavior, independent of the yield function, F .

In classical plasticity, the yield condition of a material is expressed through a surface in the stress space. Although formulation in strain-space has been proposed by various researchers such as Iwan and Yoder, Naghdi and Trapp, and Schapery, it is the classical concept that is being used extensively (Hashmi, 1987). In here, a yield function is expressed in terms of the state of stress, while the evolution or strain hardening process is characterized by using internal state variables such as the irreversible strain.

3.2 Assumptions

Every constitutive equation is generally based on some simplified assumptions and its application is also limited to a certain class of materials. In the present study, the following assumptions are made for the formulation of the elastoplastic constitutive model:

- i. The material is isotropic, and remains so during the plastic deformation.
- ii. Unloading and reloading during the deformation process are elastic.
- iii. The rate of loading is slow enough to disregard the inertia effects. Thus, the problem can be considered as quasi-static.
- iv. The system under consideration is in an isothermal condition. So temperature does not enter into the constitutive equations as an explicit state variable.
- v. Deformations are small enough to disregard the nonlinear terms in the strain displacement relations; that is, no geometric nonlinearity is considered in the formulation of the constitutive theory.
- vi. As deformations are assumed small, elastic and plastic deformations are uncoupled; thus, the total deformation at any point can be linearly decomposed into elastic and plastic parts.

3.3 Polynomial Representation of Yield Functions

A polynomial representation of a yield function in terms of certain powers of the stress invariants was originally proposed by Desai (1980). It was shown that a great many of the available yield criteria, both classical and recent, are derivable from this polynomial concept. The method proposed by Desai (1980) can provide significant flexibility in terms of choosing appropriate yield conditions for plasticity based constitutive laws.

The behavior of materials in general is influenced, among other factors, by the state of stress; state of stress is often defined by using invariants, J_1 , J_2 , and J_3 of the stress tensor, σ_{ij} . For some materials, it can be assumed that the constitutive behavior is affected by J_1 or J_2 or both; invariants J_1 and J_2 being relevant to volumetric and deviatoric behavior of a medium. For example, behavior of saturated clay may not be influenced significantly by J_1 .

Most classical criteria such as Von Mises and Drucker – Prager, include the influence of J_1 and J_2 , whereas the influence of J_3 is usually not directly incorporated in the definitions of many yield or failure criteria.

It is believed that the influence of all the three invariants should be included in yield, failure and plastic potential functions for geological media.

Consider a function F expressed as a (complete) polynomial in terms the three invariants J_1 , J_2 , and J_3 of the stress tensor, σ_{ij} :

$$\begin{aligned}
 F(J_1, J_2, J_3) = & \alpha_0 + \alpha_1 J_1 + \alpha_2 J_2^{1/2} + \alpha_3 J_3^{1/3} + \alpha_4 J_1^2 + \\
 & \alpha_5 J_1 J_2^{1/2} + \alpha_6 (J_2^{1/2})^2 + \alpha_7 J_2^{1/2} J_3^{1/3} + \alpha_8 (J_3^{1/3})^2 + \\
 & \alpha_9 J_1 J_3^{1/3} + \alpha_{10} J_1^3 + \alpha_{11} J_1^2 J_2^{1/2} + \alpha_{12} J_1 (J_2^{1/2}) + \\
 & \alpha_{13} (J_2^{1/2}) + \alpha_{14} (J_2^{1/2})^2 J_3^{1/3} + \alpha_{15} J_2^{1/2} (J_3^{1/3})^2 +
 \end{aligned}$$

$$\alpha_{16} (J_3^{1/3})^3 + \alpha_{17} J_1 (J_3^{1/3})^2 + \alpha_{18} J_1^2 J_3^{1/3} + \dots$$

(3.1)

Note:

- $\alpha_0, \alpha_1, \dots, \alpha_{18}, \dots$ are parameters and can be functions of the state of stress and physical state of the body.
- It is possible to express F as a complete polynomial by using other parameters such as strain and density as independent coordinates in addition to $J_1, J_2,$ and J_3 . However, at this time, it is assumed that the dependence of F on strain and density can be included in the functional representation for the α 's. It is also assumed at this time that the material is isotropic.
- The function F can also be expressed in terms of $J_1, J_{2D}^{1/2},$ and $J_{3D}^{1/2}$ where the later two are the second and third invariants of the deviatoric stress tensor.
- Many of the yield criteria in plasticity are specialized polynomial functions.
- It is postulated that F in Eq. (3.1) can be truncated by retaining terms and many of the resulting expressions can be used as yield, failure and potential functions. Physically, such truncations would imply an assumption that the material behavior is influenced only by the invariants of particular order retained in the truncated forms. Obviously, these propositions would require proof and verifications from observed laboratory test data.
- All combinations from Eq. (3.1) may not be suitable.

In general, as a geological material is loaded and yields plastically, the values of F will vary. Thus before failure, F can define progressing yielding. At failure F can have an invariant value. At failure or ultimate states, $\alpha_0, \alpha_1, \dots, \alpha_{18}, \dots$ would reach values corresponding to the critical values of the parameters such as density and void ratio.

Plastic potential function, Q, to describe post-yield and post-failure behavior can also be expressed in forms similar to the yield criteria.

Detailed discussion on the choice of a particular yield function from the general polynomial expression to characterize the behavior of a general class of materials can be found in the work of Faruque (1983) and Desai and Faruque (1983).

3.4 The Model

The yield function proposed here is of the form given below(Desai, 1980).

$$F = J_{2D} - F_b F_s = 0 \quad (3.2)$$

Here F_b controls the shape of the yield surface in the $J_1 - \sqrt{J_{2D}}$ space and F_s controls the shape in the octahedral plane.

$$F_b = (-\alpha J_1^n + \gamma J_1) \quad (3.2a)$$

$$F_s = (1 - \beta S_r)^m \quad (3.2b)$$

where

$$S_r = \frac{J_{3D}^{1/3}}{J_{2D}^{1/2}} \quad (3.2c)$$

Eq. (3.2a), which governs the shape of the yield surface on the $J_1 - J_{2D}$ space, can be specialized to represent the failure envelope by substituting $\alpha = 0$. The value of m is found to be -0.5 for many geologic materials.

Now Eq. (3.2) can be written as

$$J_{2D} - (-\alpha J_1^n + \gamma J_1^2)(1 - \beta S_r)^{-1/2} = 0 \quad (3.3)$$

α , β , γ and n are material response functions. Explicit forms of all the response functions are difficult to choose. Thus, only a few of the response functions will be made history dependent and the remaining will be treated as material constants. In this work, α is made a function of the deformation history while β , γ and n are material constants. It may be noted that β and γ are evaluated from the ultimate strength of a material, while n is found based on the phase change from contraction to dilation.

The evolution or growth function α can be made a function of a single parameter, ξ , defined as

$$\xi = \int (d\epsilon_{ij}^p d\epsilon_{ij}^p)^{1/2}$$

where $d\epsilon_{ij}^p$ is the plastic strain tensor in the nine dimensional strain space, and ξ is the trajectory of the plastic strains. Since the product of two vectors is a scalar and is always positive (provided the coefficients are real), the growth function ξ is always positive. Also, ξ will be unique for a particular deformed state of the material. The total plastic strain trajectory, ξ , may be expressed in terms of spherical and deviatoric components, ξ_v and ξ_D , respectively. Their relation can be expressed as

$$\xi = \int \left\{ (d\xi_D)^2 + (d\xi_v)^2 \right\}^{1/2} \quad (3.4)$$

where

$$d\xi_D = (de_{ij}^p de_{ij}^p)^{1/2}$$

$$d\xi_v = \frac{1}{\sqrt{3}}(d\epsilon_{kk}^p)^{1/2}$$

$de_{ij}^p = d\epsilon_{ij}^p - \frac{1}{3}d\epsilon_{kk}^p\delta_{ij}$ is the incremental deviatoric plastic strain tensor and $d\epsilon_{kk}^p$ is the incremental volumetric plastic strain. Thus, ξ_v and ξ_D can be expressed as

$$\xi_v = \frac{1}{\sqrt{3}} \int (d\epsilon_{kk}^p)^{1/2}$$

(3.5)

$$\xi_D = \int (de_{ij}^p de_{ij}^p)^{1/2}$$

(3.6)

It may be noted that the combinations of ξ , ξ_v , and ξ_D will form a better basis compared to ξ alone to describe the growth function α for plastically hardening materials.

The hardening function, α , is of the form

$$\alpha = \beta_a e^{-\eta_1 \xi \left(1 - \frac{\xi_D}{\beta_b + \eta_2 \xi_D}\right)}$$

(3.7)

where β_a , η_1 , β_b and η_2 are the four material constants required to describe the hardening behavior.

Characteristic of the Yield Function

The yield function may be viewed as a closed surface in the nine dimensional stress hyperspace. When Drucker's definition of stable material is considered, the yield surfaces must plot as convex surfaces. In other words, when this plasticity theory is adopted, the yield surfaces must be convex for all ranges of loadings in the plastic state.

Since nine dimensional plots are impracticable, a number of two-dimensional subspaces are chosen to verify the convexity of the proposed yield surface. Plot of the yield equation on the following spaces must be convex:

- $J_1 - \sqrt{J_{2D}}$
- Octahedral plane (3D-plane: $\sigma_1 - \sigma_2 - \sigma_3$)
- Triaxial plane ($\sigma_1 - \sqrt{2}\sigma_2 = \sqrt{2}\sigma_3$)

Fig. 3.1 shows plots of the yield function on $J_1 - \sqrt{J_{2D}}$ space. It can be seen that the function plots convex.

Fig. 3.2 shows that the yield function plots convex in the triaxial plane.

Properties of the Material Parameters

The proposed yield surface is convex in the stress space when the following restrictions are placed upon the material constants:

$$\alpha > 0, \gamma > 0, \beta < 1.375$$

CHAPTER 4

DETERMINATION OF MATERIAL CONSTANTS

4.1 General

The material constants that are associated with the model discussed herein are found based on four different states of a material deformation process: the elastic, plastic

accompanied by hardening, phase change from contraction to dilation and the ultimate state. The total number of parameters required to calibrate the model can be classified as

- i) Elastic constants: E and ν
- ii) Constants related to the ultimate state: γ , β , m
- iii) Constant related to the phase change: n
- iv) Constants related to the hardening process

4.2 Soil Testing Program

Determination of the various material constants related to a constitutive model requires broad based carefully conducted laboratory tests with a number of loading, unloading reloading cycles and physical conditions. The types of tests to be performed are governed by the material characteristics, loading conditions and availability of testing facilities.

The parameters obtained for a model based on various stress paths will be more representative of the field conditions as opposed to the conventional triaxial tests. However, values of the constants from the CTC tests are not far from the weighted averages of different loading paths and hence use of parameters from the hydrostatic compression, HC, (or consolidation) test and CTC test can provide acceptable estimates of the parameters (Desai and Faruque, 1984).

In here, the laboratory test results obtained from CTC test will be used to determine the material parameters since other testing facilities are not available. The results from the isotropic consolidation stage of the CTC test will be taken to represent HC tests.

Consolidated-Undrained (CU) tests under different confining pressures were conducted and the results are plotted as stress-strain curves. The results from the tests are as shown

together with the results from the model prediction in figures 5.1 to 5.9. Corresponding pore pressure Vs. axial strain plots are shown in the appendix.

The soil sample was collected from Addissu Gebeya area at a depth of 1.5m as undisturbed soil sample. The following are some of the properties of the soil sample:

Moisture content = 30%

Specific gravity = 2.7

It has been shown in the M.Sc. thesis work of Tadesse S. (1989) that the stress-strain response of soil samples from Addissu Gebeya, Kolfe and Rufael area of Addis Ababa are somewhat similar. Therefore the model parameters determined in this work, though developed from samples from Addissu Gebeya area, can be taken to be representative values as model parameters for the red clay soils of Addis Ababa.

4.3 Procedure for Evaluating Material Constants

4.3.1 Elastic Constants: E, ν

In the case of an isotropic material, there are two elastic constants, Young's modulus E and Poisson's ratio ν . Since the unloading-reloading phase of the deformation process is assumed to be elastic, so the 'elastic constants' can be found from the unloading-reloading curves for a given stress path. Here results from only hydrostatic and CTC stress paths are used to determine the constants E and ν . When a hydrostatic test is plotted as mean pressure V_s volumetric strain, the slope of the unloading-reloading curve will give the bulk modulus k, which can be related to E and ν through

$$k = \frac{E}{3(1 - 2\nu)} \quad (4.1)$$

For a conventional triaxial compression test (CTC) path, a plot of deviatoric stress $(\sigma_1 - \sigma_3)$ Vs deviatoric strain $2(\varepsilon_1 - \varepsilon_3)$ can be made. The slope of the unloading-reloading curve gives the shear modulus G , which can be expressed as

$$G = \frac{E}{2(1 + \nu)} \quad (4.2)$$

Using Eqs. (4.1) and (4.2), the elastic constants E and ν can be found.

Another method to obtain E and ν is to use the CTC test only. Here a plot of the deviatoric stress $(\sigma_1 - \sigma_3)$ Vs ε_1 and ε_3 is made. The slope of the unloading-reloading curve for the plot $(\sigma_1 - \sigma_3)$ Vs ε_1 gives the Young's modulus, E . While the slope of the unloading-reloading curve for the plot $(\sigma_1 - \sigma_3)$ Vs ε_3 gives E/ν . Hence, dividing the slope of the first curve with that of the second gives the Poisson's ratio ν .

To consider the effect of all stress paths into the determination of E , it is better to find the value of E from each stress path and then adopt a weighted average value. Depending on the need, it may also be possible to express E as a function of the confining (mean) pressure.

In developing this model, E is approximated as the slope of the initial linear portion of the stress-strain curve from the triaxial test result. Average value of E from triaxial tests carried out under different confining pressures is taken. The value of ν is assumed to be 0.3.

4.3.2 Ultimate State Parameters: γ , β , m

The yield function, as expressed in Eq. (3.3), when specialized to the ultimate state by substituting $\alpha = 0$, reduces to (with $m = -0.5$ observed for many geologic materials)

$$J_{2D} - (\gamma J_1^2)(1 - \beta S_r)^{-1/2} = 0 \quad (4.3)$$

which can further be expressed as

$$\frac{\sqrt{J_{2D}}}{J_1} = \frac{\sqrt{\gamma}}{(1 - \beta S_r)^{1/4}} \quad (4.4)$$

According to Eq. (4.4), two parameters, γ and β , are required to define the ultimate state of a material. Therefore, at least two tests are required to determine γ and β . If a total of N tests are used, then a system of N linear equations in two unknowns is obtained. A least squares technique is then used to evaluate γ and β . The following steps are involved in evaluating γ and β :

- i) Determination of the principal stresses, σ_1 , σ_2 , and σ_3 at the ultimate yield from all the available tests.
- ii) Calculation of J_1 and $\sqrt{J_{2D}}$ from σ_1 , σ_2 , and σ_3 , for every test
- iii) Expressing Eq. (4.4) as

$$[A]\{X\} = \{C\} \quad (4.5)$$

where $[A]$ is a $(N \times 2)$ matrix; $\{X\}$ is a (2×1) column vector and $\{C\}$ is a $(N \times 1)$ column vector; N is the number of tests.

Coefficients of $[A]$ are defined as $a_{i1} = \left(\frac{J_{2D}^2}{J_1^4} S_r \right)_i$; $a_{i2} = 1$.

Coefficients of $\{C\}$ are defined as $C_i = \frac{J_{2D}^2}{J_1^4}$; i refers to the test number.

The vector $\{X\} = \begin{Bmatrix} \gamma \\ \beta \end{Bmatrix}$

To obtain γ and β from Eq. (4.5), two tests are required. In general, $N > 2$, so the system of equations is overdeterminate. Hence, a least-squares technique is used to obtain γ and β .

4.3.3 Phase Change Parameter: n

The value of n can be determined from the state of stress (in the experiment) at which the rate of volume change is zero. At this state, from Eq. (3.3)

$$\frac{J_{2D}}{J_1^2} = (-\alpha J_1^{n-2} + \gamma) F_s \quad (4.6)$$

Also, at zero volume change

$$\frac{\partial F}{\partial J_1} = 0 \quad (4.7)$$

which yields

$$\alpha = \frac{2\gamma}{nJ_1^{n-2}} \quad (4.8)$$

Using Eqs.(4.7) and (4.8), n can be expressed as

$$n = \frac{2}{1 - \frac{J_{2D}}{J_1^2 \gamma (1 - \beta S_r)^{-1/2}}} \quad (4.9)$$

So, by noting the point of phase change from experiment, corresponding values of J_1 and J_{2D} can be obtained. These values are substituted into Eq. (4.9) to obtain n .

The value of n can also be determined from hydrostatic compression (HC) tests using the following relation specialized for HC test.

$$d\varepsilon_{ii}J_1^{n-1} = \sqrt{3}\gamma dJ_1(n-2)$$

(4.10)

At any state in the (HC) experiments, the first invariant of stresses J_1 , the increment of J_1 , dJ_1 and the increment of volumetric strain $d\varepsilon_{ii}$ are known. Then n can be obtained by using Eq. (4.10).

From experimental data, it is observed that for many relatively dense materials the value of n lies between 3 and 4. Then an assumed value of n , e.g. $n=3$, would be a significant simplification (Desai, Frantzikonis, Somasundaram, 1986). For this model an assumed value of $n = 3$ is used.

4.3.4 Constants for Hardening

The hardening function, α , as pointed out earlier, is of the form

$$\alpha = \beta_a e^{-\eta_1 \xi \left(1 - \frac{\xi_D}{\beta_b + \eta_2 \xi_D}\right)}$$

(4.11)

where β_a , η_1 , β_b and η_2 are the four material constants required to describe the hardening behavior. Since the deformation process is influenced by the coupled action of hydrostatic and deviatoric stresses, the constants are determined based on stress paths that account for this influence.

Determination of β_a and η_1 : When an initially isotropic material is subjected to a pure hydrostatic state of stress, it only undergoes volumetric strains. So the deviatoric strains are equal to zero. Hence, ξ_D , which is the trajectory of the deviatoric part of the total plastic strain, is also zero, and Eq. (4.11) reduces to

$$\alpha = \beta_a e^{-\eta_1 \xi_v} \quad (4.12)$$

Taking the natural logarithm of both sides of Eq. (4.12) yields

$$\ln(\alpha) = \ln(\beta_a) - \eta_1 \xi_v \quad (4.13)$$

Equation (4.13) can be plotted for $\ln(\alpha)$ vs. ξ_v and a straight line can be fitted through the points. Then β_a and η_1 are obtained from the intercept and slopes of the straight line, respectively. A detailed stepwise description for evaluating β_a and η_1 is given below.

- i) From an HC test, a plot of mean pressure p vs. volumetric strain, ε_v , is made. A number of points, say N , are chosen on the test curve and ξ_v is calculated as

$$\xi_v = \frac{1}{\sqrt{3}} \sum_{i=1}^N \Delta^i \varepsilon_v^p$$

where $\Delta^i \varepsilon_v^p$ denotes the i^{th} incremental volumetric plastic strain.

- ii) The magnitude of the growth function corresponding to each of the N points chosen above can be found by specializing the yield function, Eq. (3.3), to the hydrostatic state of stress. This yields

$$F = \alpha J_1^n - \gamma J_1^2 = 0$$

(4.15)

Since γ and n have already been obtained from the ultimate and phase change conditions, the growth function, α , can then be expressed as

$$\alpha = \gamma J_1^{n-2}$$

(4.16)

- iii) For each of the N points, $\ln(\alpha)$ is calculated using Eq. (4.16), and a plot of $\ln(\alpha)$ vs. ξ_v is obtained.
- iv) A straight line is drawn through these points. The slope of this straight line gives constant, η_1 , while the intercept with the $\ln(\alpha)$ axis represents $\ln(\beta_a)$, from which β_a can be computed.

Determination of β_b and η_2 : Having obtained β_a and η_1 , Eq.(4.11) can be modified by taking natural logarithm of both as

$$\ln(\alpha) = \ln(\beta_a) - \eta_1 \xi \left(1 - \frac{\xi_D}{\beta_b + \eta_2 \xi_D}\right)$$

(4.17)

Equation (4.17) can be simplified as

$$\frac{\xi_D}{\beta_b + \eta_2 \xi_D} = 1 + \frac{\ln(\alpha) - \ln(\beta_a)}{\eta_1 \xi}$$

(4.18)

Equation (4.18) can now be written as

$$\frac{\xi_D}{\beta_b + \eta_2 \xi_D} = h \quad (4.19)$$

where

$$h = 1 + \frac{\ln(\alpha) - \ln(\beta_a)}{\eta_1 \xi} \quad (4.20)$$

Equation (4.18) can further be rearranged and expressed in the form of a straight line as

$$\frac{\xi_D}{h} = \beta_b + \eta_2 \xi_D \quad (4.21)$$

The intercept and slope of the above line gives β_b and η_2 , respectively.

The following steps are involved in the evaluation of β_b and η_2 . Although results from various stress paths are used to find the constants β_b and η_2 , here only CTC test will be used to explain the procedure involved.

- i) The stress-strain curve for a CTC test is plotted. A number of points N are chosen on this curve. Corresponding to each point, the elastic strain is found by dividing the stress by the unloading modulus. The plastic strains, ϵ_i^p ($i = 1, 2, 3$) are obtained by subtracting the elastic strains from the total strains at each point. Here, the superscript p denotes plastic strain. From ϵ_i^p ($i = 1, 2, 3$), the incremental plastic strains, $\Delta\epsilon_i^p$, between two adjacent points are obtained.
- ii) At every point, $\Delta\xi$ and $\Delta\xi_D$ are then calculated from the total incremental plastic strains, $\Delta\epsilon_i^p$.

$$\Delta\xi = \left[(\Delta\varepsilon_1^p)^2 + (\Delta\varepsilon_2^p)^2 + (\Delta\varepsilon_3^p)^2 \right]^{1/2}$$

(4.22)

$$\Delta\xi_D = \left[(\Delta e_1^p)^2 + (\Delta e_2^p)^2 + (\Delta e_3^p)^2 \right]^{1/2}$$

(4.23)

where

$$\Delta e_{ij}^p = \Delta\varepsilon_{ij}^p - 1/3\Delta\varepsilon_{kk}\delta_{ij}$$

(4.24)

iii) Total ξ and ξ_D at the r^{th} point are then calculated according to the following equations:

$$\xi^r = \xi_o + \sum_{i=1}^r \Delta\xi^i$$

and

$$(4.25)$$

$$\xi_D^r = \sum_{i=1}^r \Delta\xi_D^i$$

where r refers to the point at which the quantities are calculated, $\Delta\varepsilon^i$ and $\Delta\varepsilon_D^i$ in Eq.(4.25) denote the i^{th} increments of ξ and ξ_D , respectively. ξ_o is the value of ξ corresponding to the initial confining pressure, σ_o , at which shearing started.

- iv) The stress invariants J_1 , J_{2D} , and J_{3D} are computed at each of the N points from the known stresses.
- v) The magnitude of α is calculated from the expression

$$\alpha = \gamma J_1^{n-2} - \frac{J_{2D}}{J_1^2} (1 - \beta S_r)^{-1/2}$$

(4.26)

- vi) For each of the N points, h is calculated using relation Eq.(4.20). Then ξ_D / h is plotted with respect to ξ_D .
- vii) A straight line is drawn through the points. The slope of the line provides η_2 while the intercept with ξ_D / h gives the value of β_b .

4.4 Material Constants for the Red Clay Soils of Addis Ababa

Based on the procedures discussed in this chapter the values of the material constants obtained are:

$$\gamma = 1.375$$

$$\beta = 1.200$$

$$\eta_1 = 125.810$$

$$\beta_a = 244.000$$

$$\eta_2 = 0.959$$

$$\beta_b = 0$$

CHAPTER 5

VALIDATION OF THE MODEL

5.1 General

The acceptance of a constitutive model to describe a material behavior will fall short if its capability of predicting observed material behavior is not properly tested.

The proposed model has to be validated:

1. By back predicting observed stress-strain response curves for different tests which were used to find the material constants; and
2. By predicting observed stress-strain curves that were not used for finding the material constants.

5.2 Model Validation

The procedure for the validation is as follows:

- i) J_1 , J_{2D} , and J_{3D} (and hence S_r) can be computed for a given state of stress defined by σ_1' , σ_2' , and σ_3' . These together with the known material parameters γ and β can be used to determine the growth function α using Eq. (4.26).
- ii) ξ is computed from equations (4.20) and (4.21) by using the already determine material parameters β_a , η_1 , β_b , and η_2
- iii) From the value of ξ computed the incremental plastic strains could be computed using Eq. (4.23).
- iv) The elastic components of the strains are obtained from the state of stress and the elastic constants.
- v) The total strain is then equal to the sum of the elastic and plastic components.

The results from the procedure described are plotted as stress-strain curves. The comparison of the results from laboratory testing and the model prediction are as shown from figure 5.1 to 5.9.

Conclusions and Recommendations

A model developed by Desai was proposed and verified for the red clay soils of Addis Ababa. The significant parameters of the model were identified and the material constants were determined from stress-strain responses. Validation of the model was carried out by back predicting the stress-strain responses of the laboratory tests used to find the parameters. Stress-strain responses that were not used to find the material constants were also predicted.

It can be seen that there is a difference between the laboratory and the model stress-strain curves in the initial linear portions of this curves. This deviation is due to the approximate value used for the Young's modulus of elasticity.

Conclusions

1. Comparison of observed and predicted response for the red clay soils of Addis Ababa soils shows that the model yielded predictions that compared remarkably well with the observed behavior.
2. The model, after being refined by conducting different stress-path tests, can be incorporated into finite element codes and used in analyzing soil-structure interaction problems.

Recommendations

1. A new model can be developed by choosing appropriate yield conditions from the general equation proposed by Desai, Eq.(3.1). This needs laboratory tests carried out under different stress paths. Therefore, this can be considered in future works.
2. In this work only the basic isotropic hardening associative model (δ_0) of the HISS has been considered. It will be good if the parameter for the nonassociative case is determined and comparison of the two cases is made.
3. If in the future the laboratory facilities are to improve, it would be good to refine the model by conducting different stress-path tests and check the model's prediction capacity under a variety of stress paths.
4. In this work the soil parameters were determined using samples from Addissu Gebeya. It is recommended that the material constants be determined from tests conducted on samples from other parts of Addis Ababa and the results compared with those in this work.
5. The same model can be extended to other soil types with appropriate modifications.

LIST OF REFERENCES

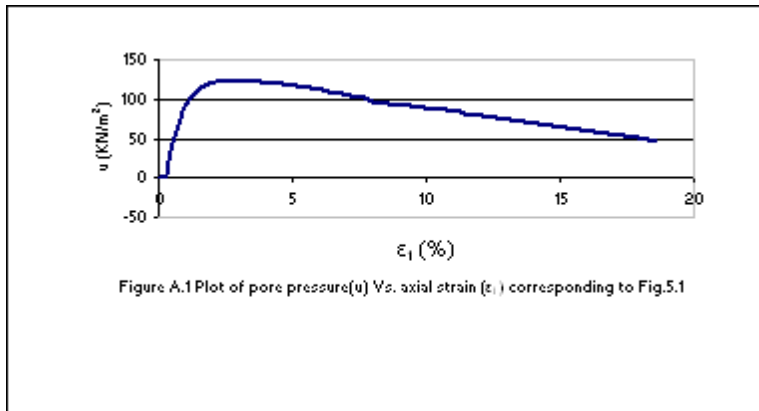
1. Chen, W.F. and Mizuno, E., "Nonlinear Analysis in Soil Mechanics – Theory and Implementation," Elsevier, New York, 1990.
2. Desai, C.S., " A general Basis for Yield, Failure and Potential Functions in Plasticity," Int. J. Num. Analyt. Meth. In Geomech., Vol. 4, 1980, pp. 361 – 375.
3. Desai, C.S. and Gioda,G., "Numerical Methods and Constitutive Modelling in Geomechanics," CISM Courses and Lectures No. 311, International Center for Mechanical Sciences, 1990.
4. Desai, C.S. and Fruque, M.O., "Constitutive Model for Geologic Materials," J. Engg. Mech. Div., ASCE, Vol. 110, No. 9, September 1984, pp. 1391 – 1408.
5. Desai, C.S., Somasundaram, S. and Frantziskonis, G.N., "A Hierarchical Approach for Constitutive Modelling of Geologic Materials," Int. J. Num. Analyt. Meth. In Geomech., Vol. 10, 1986, pp. 225 – 257.
6. Faruque, M.O. and Desai, C.S., "Implementation of a General Constitutive Model for Geological Materials," Int. J. Num. Analyt. Meth. In Geomech., Vol. 9, No. 5, 1985, pp. 415 – 436.
7. Fratziskonis, G.N., Desai, C.S. and Somasundaram, S., " Constitutive Model for Nonassociative Behavior," J. of Engg. Mech., ASCE, Vol. 112, No. 9, September 1986, pp. 932 – 946.
8. Pastor, M., Zienkiewicz, O.C. and Chan, H.C., "Generalized Plasticity and the Modelling of Soil Behavior," Int. J. Num. Analyt. Meth. In Geomech., Vol. 14, 1990, pp. 151 – 190.

9. Tadesse, S., “ Investigation into some of the Engineering Properties of Addis Ababa Red Clay Soils,” M.Sc. Thesis, Addis Ababa University, Addis Ababa, 1989.

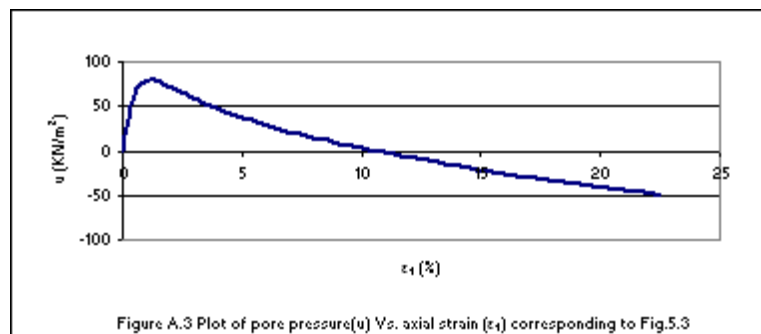
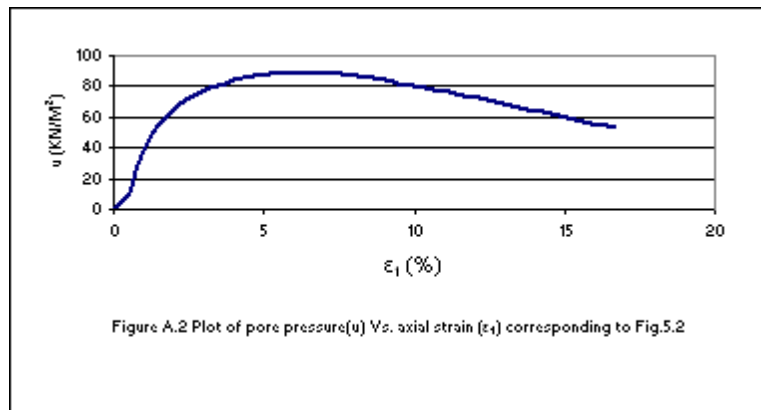
10. Hashmi, Q.S.E., “Nonassociative Plasticity Model for Cohesionless Materials and Its Implementation in Soil-structure Interaction,”Ph. D. Dissertation, University of Arizona, Tucson, Arizona, 1987.

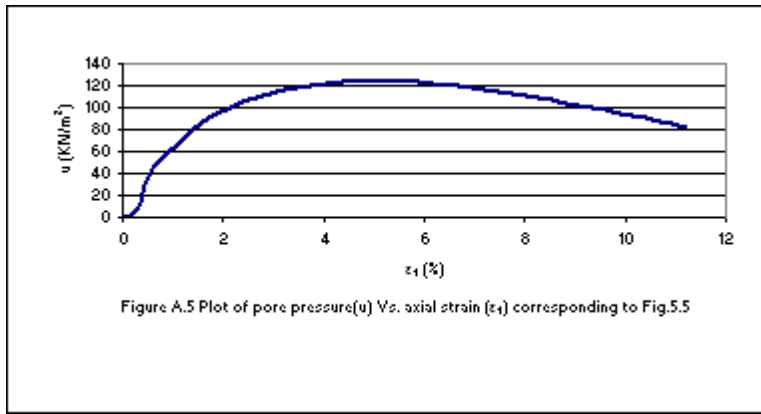
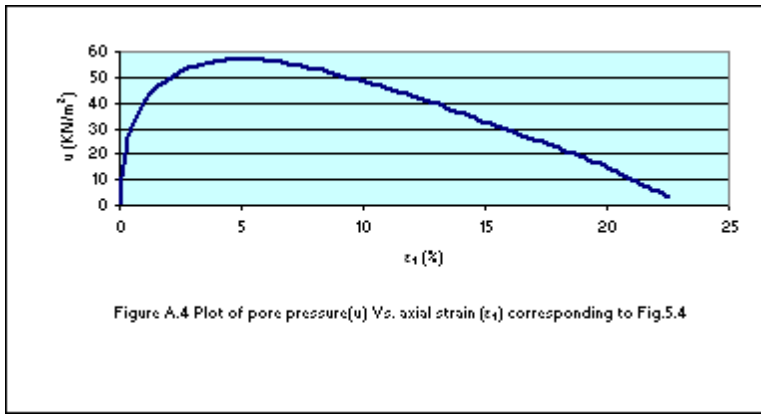
11.

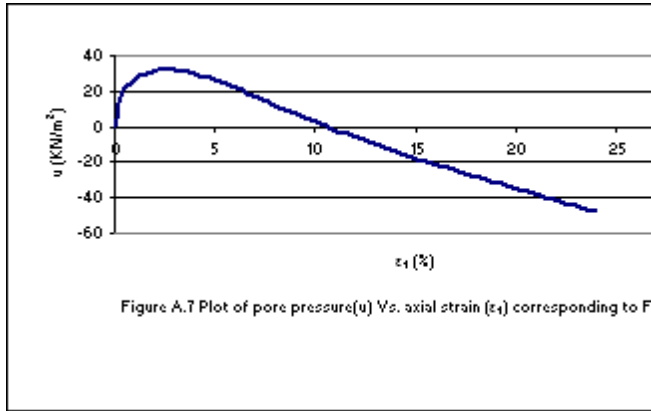
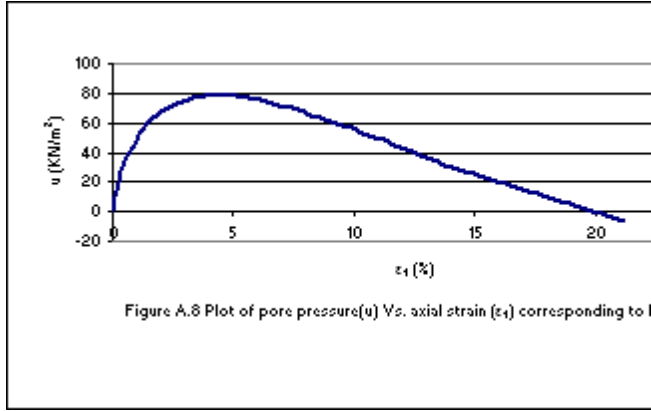
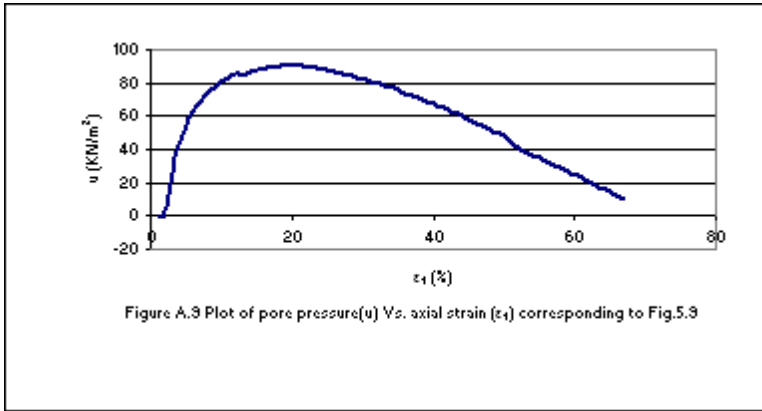
12.



ϵ







69

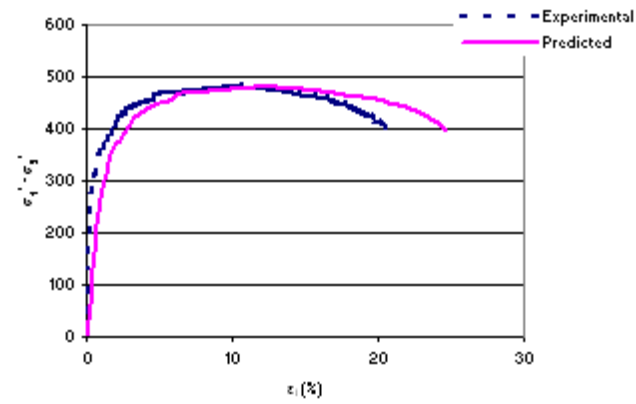


Figure 5.6 Comparison of stress-strain curves for a test ($\sigma_3' = 130\text{KPa}$) not used to find the material constants

60

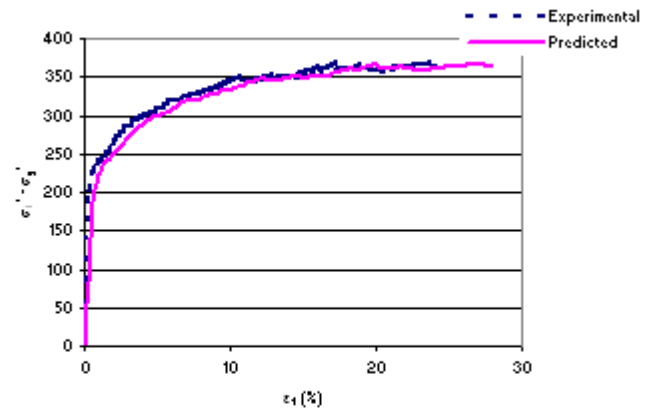


Figure 5.7 Comparison of stress-strain curves for a test ($\sigma_3' = 110\text{KPa}$) not used to find the material constants

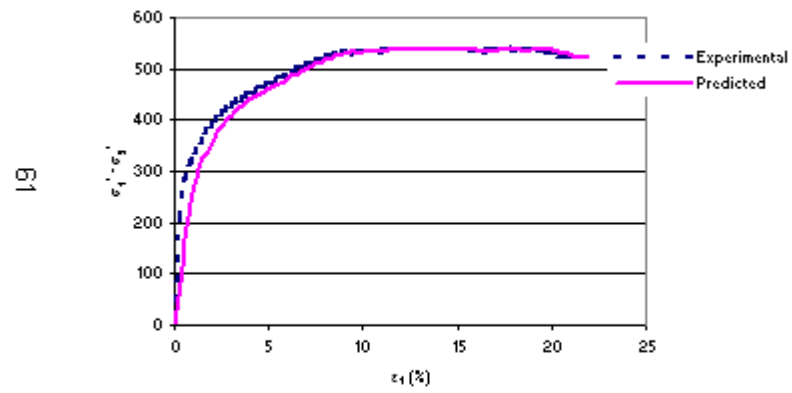
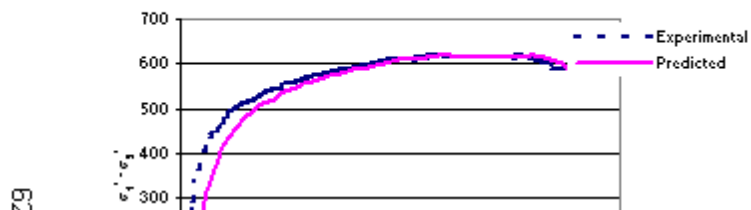
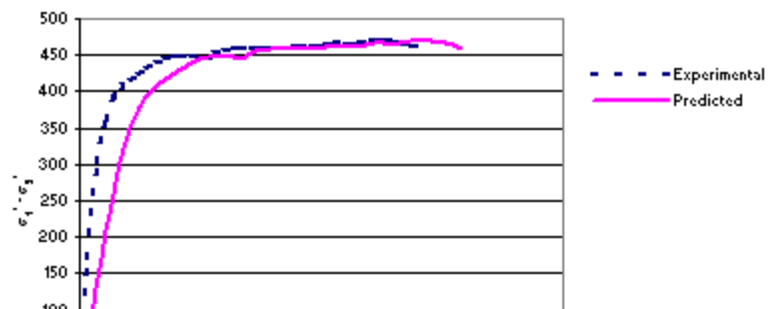


Figure 5.8 Comparison of stress-strain curves for a test ($\sigma'_v = 130\text{KPa}$) not used to find the material constants.





Computations to show that the yield function plots convex in the stress space

j1	j2d	sqrt(j2d)	alpha=0.02		alpha=0.03		Sigma 3	sigma3	Sigma 1	sigma1	roos2*sig2
0	0	0	0	0	0	0	0	0	0	0	0
5	92.91875	9.639437	89.4125	9.455818	85.90625	9.268562	7.231998	-3.89867	12.79733	-9.464	10.22759
15	773.15625	27.80569	678.4875	26.04779	583.8188	24.16234	21.05362	-11.0536	37.10724	-27.1072	29.77432
20	1318.4	36.30978	1094	33.07567	869.6	29.48898	27.63013	-14.2968	48.59359	-35.2603	39.0749
25	1972.3438	44.41108	1534.063	39.16711	1095.781	33.10259	33.97408	-17.3074	59.61483	-42.9482	48.04661
30	2713.95	52.09559	1956.6	44.23347	1199.25	34.63019	40.0774	-20.0774	70.1548	-50.1548	56.678
35	3522.1813	59.34797	2319.538	48.16158	1116.894	33.41996	45.93123	-22.5979	80.1958	-56.8625	64.95657
40	4376	66.15134	2580.8	50.80157	785.6	28.02856	51.52583	-24.8592	89.71832	-63.0517	72.86853
45	5254.3688	72.48702	2698.313	51.94528	142.2563	11.92712	56.8504	-26.8504	98.70081	-68.7008	80.39861
50	6136.25	78.33422	2630	51.28353	-876.25	#NUM!	61.89295	-28.5596	107.1192	-73.7859	87.52985
55	7000.6063	83.66963	2333.788	48.30929	-2333.03	#NUM!	66.64001	-29.9733	114.9467	-78.28	94.24321

60	7826.4	88.46694	1767.6	42.04284	-4291.2	#NUM!	71.07641	-31.0764	122.1528	-82.1528	100.5172
65	8592.5938	92.69624	889.3625	29.82218	-6813.87	#NUM!	75.18487	-31.8515	128.7031	-85.3697	106.3275
70	9278.15	96.32315	-343	#NUM!	-9964.15	#NUM!	78.94553	-32.2789	134.5577	-87.8911	111.6458
75	9862.0313	99.30776	-1971.56	#NUM!	-13805.2	#NUM!	82.33536	-32.3354	139.6707	-89.6707	116.4398
80	10323.2	101.6031	-4038.4	#NUM!	-18400	#NUM!	85.32727	-31.9939	143.9879	-90.6545	120.671
85	10640.619	103.1534	-6585.59	#NUM!	-23811.8	#NUM!	87.88896	-31.2223	147.4446	-90.7779	124.2938
90	10793.25	103.8906	-9655.2	#NUM!	-30103.7	#NUM!	89.98125	-29.9812	149.9625	-89.9625	127.2527
95	10760.056	103.7307	-13289.3	#NUM!	-37338.7	#NUM!	91.55561	-28.2223	151.4446	-88.1112	129.4792
100	10520	102.5671	-17530	#NUM!	-45580	#NUM!	92.55045	-25.8838	151.7676	-85.1009	130.8861
105	10052.044	100.2599	-22419.3	#NUM!	-54890.7	#NUM!	92.88507	-22.8851	150.7701	-80.7701	131.3593
110	9335.15	96.61858	-27999.4	#NUM!	-65334	#NUM!	92.44943	-19.1161	148.2322	-74.8989	130.7432
115	8348.2813	91.36893	-34312.3	#NUM!	-76972.8	#NUM!	91.08521	-14.4185	143.8371	-67.1704	128.8139
120	7070.4	84.08567	-41400	#NUM!	-89870.4	#NUM!	88.54688	-8.54688	137.0938	-57.0938	125.2242
125	5480.4687	74.03019	-49304.7	#NUM!	-104090	#NUM!	84.40802	-1.07468	127.1494	-43.816	119.371
130	3557.45	59.64436	-58068.4	#NUM!	-119694	#NUM!	77.76902	8.897644	112.2047	-25.538	109.982
135	1280.3062	35.78137	-67733.2	#NUM!	-136747	#NUM!	65.65838	24.34162	86.31676	3.683236	92.85497
136	780.5312	27.93799	-69778	#NUM!	-140337	#NUM!	61.46334	29.20333	77.59334	13.07332	86.92229
137	265.58135	16.29667	-71860.9	#NUM!	-143987	#NUM!	55.07555	36.25778	64.48444	26.8489	77.88859
138	-264.7116	#NUM!	-73982.1	#NUM!	-147700	#NUM!	#NUM!	#NUM!	#NUM!	#NUM!	#NUM!
139	-810.51595	#NUM!	-76142.1	#NUM!	-151474	#NUM!	#NUM!	#NUM!	#NUM!	#NUM!	#NUM!
140	-1372	#NUM!	-78341.2	#NUM!	-155310	#NUM!	#NUM!	#NUM!	#NUM!	#NUM!	#NUM!

